Journal of X-Ray Science and Technology 15 (2007) 235–270
IOS Press

Scheme of computed tomography

Yuchuan Wei[a,*], Hengyong Yu[b], Jiang Hsieh[c], Wenxiang Cong[b] and Ge Wang[a,b,*]
[a]*Biomedical Imaging Division, VT-WFU School of Biomedical Engineering and Science, Wake Forest University, Winston-Salem, NC 27157, USA*
[b]*Biomedical Imaging Division, VT-WFU School of Biomedical Engineering and Science, Virginia Tech, Blacksburg, VA 24061, USA*
[c]*Laboratories of Applied Science, GE Healthcare Technologies, Milwaukee, WI 53201, USA*

Received 19 June 2007
Revised 28 August 2007
Accepted 30 August 2007

Abstract. Since Katsevich's work on cone-beam CT in 2002, a series of new reconstruction formulae for cone-beam and fan-beam reconstruction have been published. To understand these new results in a unified way, two schemes were proposed in the literature: one is based on the Radon formula, while the other on the Tuy formula. In the paper, we present a general two-step scheme for parallel-, fan- and cone-beam CT based on the inverse Fourier transform. We first derive parallel-beam formulae and then translate them to the divergent-beam case via a standardized method. This complete framework not only provides a single mechanism for the deduction of most existing CT formulae but also generates new algorithms. Meanwhile, along the development of this new framework some minor flaws are identified and fixed in publications. Additionally, the traditional assumption that an object be compactly supported inside a scanning trajectory is no longer needed.

Keywords: Computed Tomography (CT), Fourier analysis, convolution theorem, Dirac function, two-step scheme, instantaneous cylindrical system, three-step method, weighted back-projection (WBP), weighted Hilbert transform (WHT), frequency plane, dartboard function, Outward-homeward function, J function, odd/even extension, cone-beam, complete region, trajectory projection

1. Introduction

The British engineer Hounsfield reported the first x-ray computed tomography (CT) scanner in 1973, with which the internal structure of an object can be recovered from projections [1]. The invention of CT started a new era of medical imaging and nondestructive testing [2–4]. During the CT development, the imaging system has been changed from parallel-beam to fan-beam, and eventually to cone-beam geometry (see Fig. 1). The essence of the CT theory is to find formulae for image reconstruction of an object from projections collected in a beam geometry along a scanning trajectory. The Radon formula [5] is traditionally considered as the foundation of CT over several decades. The filtered backprojection (FBP) formula in the parallel-beam case, which was developed from the Fourier slice theorem [6], is equivalent to the Radon formula in the 2D case. The FBP formula in the fan-beam case was deducted from the Radon formula [7]. Some cone-beam CT formulae [8,9] were also developed from the Radon formula. Before 2002, all the exact reconstruction formulae require that the object be entirely covered by

*Corresponding authors. E-mail: ywei@gmail.com; wangg@vt.edu.

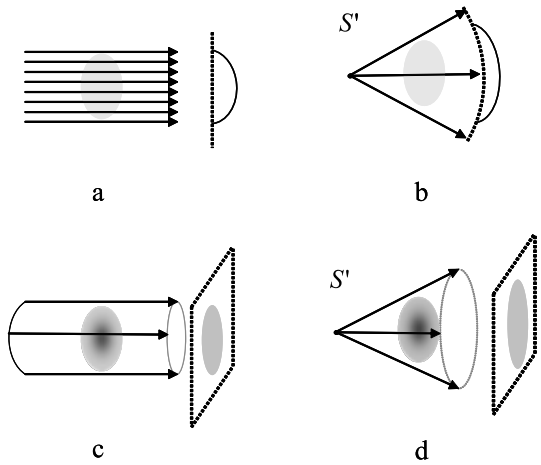

Fig. 1. Shapes of the x-ray beams and their projections on the detection plane (array). (a) A 2D parallel-beam, (b) a fan-beam, (c) a 3D parallel-beam, and (d) a cone-beam.

the x-ray beam(s). In 2002, Katsevich reported the first cone-beam formula that can exactly reconstruct an object from longitudinally truncated cone-beam projections [10,11]. Since then, a series of cone-beam formulae [12] were developed, including FBP [13–17] and backprojection filtration (BPF) [13,15,18–20] formulae. Interestingly, the rapid advancement of cone-beam CT [21] has a significant impact on the corresponding development of fan-beam and parallel-beam CT as well. In the fan-beam case, the new formulae enable the exact reconstruction of a local region from a super short scan [22,23] or from a transversely truncated dataset [24]. In the parallel-beam case, a class of non-Radon-transform-based formulae were reported [25].

The accumulation of all these impressive new results has motivated researchers to revisit the theoretical foundation of CT. One major question we have is whether we could use one fundamental formula to generate all the CT formulae recently discovered. The answer to this question will not only reveal the internal relations among the existing formulae but also suggest the new directions of the CT research. Some important advances have been made in that aspect. Katsevich [21] developed a general scheme for FBP cone-beam reconstruction based on the Radon formula. Chen et al. [23,26] and Zhao et al. [15] developed the unified schemes for divergent beam reconstruction based on the Tuy formula [27].

In this paper, our goal is to provide an intuitive and comprehensive framework based on a new and flexible two-step reconstruction formula. First, we develop various formulae in the parallel-beam case. Then, we translate them to the divergent-beam case via the relationship between the parallel and divergent projections. While our formulae are consistent with most recent findings, some hidden flaws are identified and fixed in several publications.

The paper is organized in an intuitive and self-contained manner, and goes from 2D to 3D, and from parallel- to divergent-beam cases. In Section 2, a two-step reconstruction formula for 2D parallel-beam CT is introduced, which can generate existing and new formulae for 2D parallel-beam reconstruction. In Section 3, the parallel-beam formulae are translated to fan-beam geometry. Using the 2D CT as a template, we then expand the formulae to the 3D case, in which the long object problem is also considered. In Section 4, the 3D version of the two-step reconstruction formula is introduced, which generates various formulae for truncated 3D parallel-beam projection. In Section 5, the parallel-beam formulae are translated for cone-beam CT. Finally, we conclude the paper in Section 6.

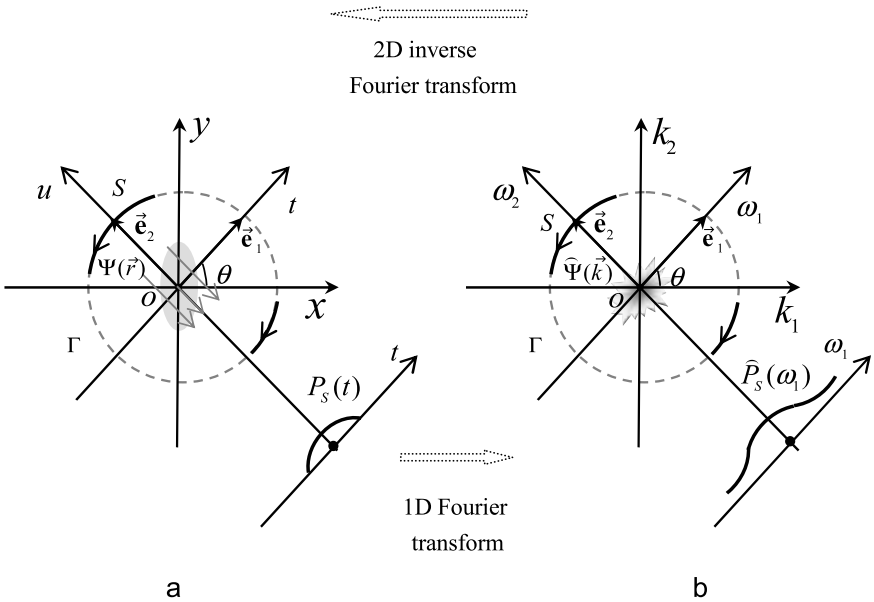

Fig. 2. 2D parallel-beam reconstruction geometry. (a) A parallel-beam projection, and (b) the Fourier transform of the projection profile in the Fourier space.

2. 2D parallel-beam reconstruction

2.1. The classical formula for 2D parallel-beam reconstruction

Let us simply recall the classical formula for 2D parallel-beam reconstruction and introduce the necessary notations [2]. In the 2D space R^2, $\Psi(\vec{r})$ is an object function to be reconstructed (see Fig. 2) whose Fourier transform is $\widehat{\Psi}(\vec{k})$. According to the Fourier theory, we have

$$\Psi(\vec{r}) = \int_{-\infty}^{\infty}\int_{-\infty}^{\infty} \widehat{\Psi}(\vec{k}) \exp(2\pi i\vec{k}\cdot\vec{r}) dk_1 dk_2 \tag{1}$$

where $\vec{r} = (x, y)$ and $\vec{k} = (k_1, k_2)$ are 2D vectors in the real space and Fourier domain, respectively. In the polar coordinate system, Eq. (1) is expressed as

$$\Psi(\vec{r}) = \int_{0}^{2\pi}\int_{0}^{\infty} \widehat{\Psi}(\vec{k}) \exp(2\pi i\vec{k}\cdot\vec{r}) k dk d\theta \tag{1a}$$

$$= \int_{0}^{\pi}\int_{-\infty}^{\infty} \widehat{\Psi}(\vec{k}) \exp(2\pi i\vec{k}\cdot\vec{r}) |k| dk d\theta. \tag{1b}$$

where the standard polar coordinate (k, θ) with $0 \leqslant k < \infty, 0 \leqslant \theta < 2\pi$ is used in Eq. (1a) while a signed polar coordinate (k, θ) with $-\infty < k < \infty, 0 \leqslant \theta < \pi$ is used in Eq. (1b). By the way, starting from (1a) a Tuy-type framework for fan-beam reconstruction was set up [23]. In the following, our discussion will be based on Eq. (1b).

The unit circle with the center origin O can be defined as

$$\Omega^1 = \left\{ S : \overrightarrow{OS} = \vec{e}_2 = (-\sin\theta, \cos\theta), \theta \in [0, 2\pi) \right\} \tag{2}$$

Based on the two orthonormal vectors $\vec{e}_1$ and $\vec{e}_2$:

$$\vec{e}_1 = (\cos\theta, \sin\theta), \;\; \vec{e}_2 = (-\sin\theta, \cos\theta). \tag{3}$$

we set up two local coordinate systems Otu and $O\omega_1\omega_2$:

$$\begin{aligned} &t = \vec{r} \cdot \vec{e}_1 \,,\; u = \vec{r} \cdot \vec{e}_2, \\ &\omega_1 = \vec{k} \cdot \vec{e}_1 \,, \omega_2 = \vec{k} \cdot \vec{e}_2 \,. \end{aligned} \tag{4}$$

The parallel-beam projection of the object along the vector $\overrightarrow{OS}$ is defined as

$$P_S(t) = P_\theta(t) = \int_{-\infty}^{\infty} \Psi(t\vec{e}_1 + u\vec{e}_2) du. \tag{5}$$

The goal of the reconstruction is to calculate the function $\Psi(\vec{r})$ from its projections $P_S(t)$, either exactly or approximately.

Based on the Fourier slice theorem [2], one has

$$\widehat{\Psi}(\omega_1\vec{e}_1) = \widehat{P}_S(\omega_1) = \int_{-\infty}^{\infty} P_S(t) \exp(-2\pi i\omega_1 t) dt. \tag{6}$$

Then, the object can be reconstructed by

$$\Psi(\vec{r}) = \int_0^{\pi} \int_{-\infty}^{\infty} \exp(2\pi i\omega_1 t) \widehat{P}_S(\omega_1) |\omega_1| d\omega_1 d\theta. \tag{7}$$

This is the classical FBP formula, which is equivalent to the Radon inversion formula [5].

2.2. The complete arcs on the unit circle

We call one arc or a union of several arcs on the unit circle Ω^1 a curve, denoted by Γ. Γ is called complete if Γ intersects any diameter of Ω^1 at least once (Fig. 3). The simplest complete curve is a half circle, called a 180° scan, i.e. $\theta \in [0, \pi)$.

In the frequency domain, for a unit vector $\overrightarrow{OS} \in \Omega^1$, let us define the frequency line

$$L(\overrightarrow{OS}) = \left\{ \vec{k} \in R^2 : \vec{k} \cdot \overrightarrow{OS} = 0 \right\}$$

which passes the origin O and is orthogonal to the vector $\overrightarrow{OS}$. In fact $L(\overrightarrow{OS})$ is the line on which the axis $O\omega_1$ is located in Fig. 2.

The completeness of a curve Γ is dependent on whether the frequency line $L(\overrightarrow{OS})$ will sweep the entire space when the point S moves along the curve Γ. Further, when S moves along a given curve Γ, the times that the frequency line $L(\overrightarrow{OS})$ sweeps a specified point $\vec{k} \in R^2$ is denoted as $J_{\vec{k}}$. Geometrically, there are $J_{\vec{k}}$ intersection points between the curve Γ and the diameter orthogonal to the point $\vec{k}$, denoted as $S^j, j = 1, 2, \ldots, J_{\vec{k}}$, as shown in Fig. 3. In the following, all the formulae are based on complete curves unless otherwise stated.

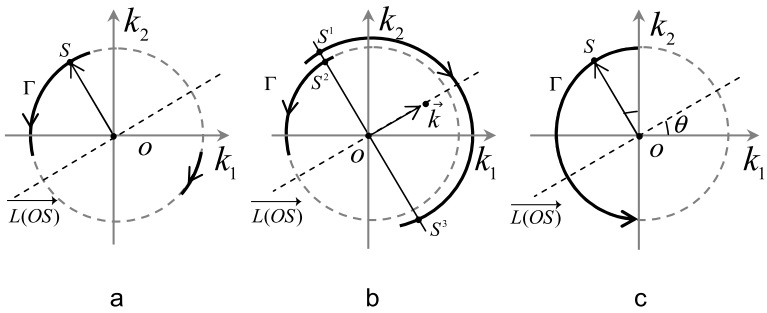

Fig. 3. Completeness of arcs on the unit circle. (a) An incomplete curve, and (b) a complete curve, and (c) a 180° scan.

2.3. The two-step reconstruction for 2D parallel-beam CT

For a complete curve Γ and a normalized weight function $w_S(\vec{k})$, an object function can be recovered by

$$\Psi(\vec{r}) = \int_\Gamma \int_{-\infty}^{\infty} w_S(\vec{k}) \exp(2\pi i \omega_1 t) \widehat{P}_S(\omega_1) |\omega_1| d\omega_1 |d\theta| \tag{8}$$

where $|d\theta|$ is the length of a different arc on Γ.

The weight function$w_S(\vec{k})$, defined for every $S \in \Gamma$ and all $\vec{k} \in L(\overrightarrow{OS})$, is used to avoid over-sampling at any frequency. Since a point $\vec{k}$ is swept by the frequency line $J_{\vec{k}}$ times, the weight function must satisfy the normalization condition $\sum_{j=1}^{J_{\vec{k}}} w_{S^j}(\vec{k}) = 1$ for all $\vec{k} \in R^2$.

For a weight function $w_S(\vec{k})$ with a general summation $w(\vec{k}) = \sum_{j=1}^{J_{\vec{k}}} w_{S^j}(\vec{k})$, we have

$$\Phi(\vec{r}) = \int_\Gamma \int_{-\infty}^{\infty} w_S(\vec{k}) \exp(2\pi i \omega_1 t) \widehat{P}_S(\omega_1) |\omega_1| d\omega_1 |d\theta|$$

$$\widehat{\Phi}(\vec{k}) = \widehat{\Psi}(\vec{k}) w(\vec{k}) \tag{9}$$

where the function $\Phi(\vec{r})$ is called an intermediate function whose Fourier transform is denoted by $\widehat{\Phi}(\vec{k})$.

Equation (9) defines a new and flexible two-step ($P_S(t) \to \Phi(\vec{r}) \to \Psi(\vec{r})$) scheme for the 2D parallel-beam CT. For a normalized weight function $w_S(\vec{k})$, we have $\Phi(\vec{r}) = \Psi(\vec{r})$since$w(\vec{k}) = 1$. For a weight function $w_S(\vec{k})$with $w(\vec{k}) \neq 0$ in any region of the frequency domain, the object can be reconstructed from the intermediate function by the second step:

$$\widehat{\Psi}(\vec{k}) = \widehat{\Phi}(\vec{k}) / w(\vec{k})$$

or equivalently

$$\Psi(\vec{r}) = \Phi(\vec{r}) * * W(\vec{r})$$

$$W(\vec{r}) = \int_{R^2} \frac{1}{w(\vec{k})} \exp(i2\pi\vec{k}\cdot\vec{r})d^2\vec{k}.$$

Here ** denotes the 2D convolution in R^2.

The inner integral in Eq. (9) is called filtered projection

$$\tilde{P}_S(t) = \int_{-\infty}^{\infty} w_S(\vec{k}) \exp(2\pi i\omega_1 t)\widehat{P}_S(\omega_1)|\omega_1|d\omega_1 \tag{10}$$

2.4. Various reconstruction formulae

There are many ways to choose the weight function, and different weight functions lead to various reconstruction formulae. To demonstrate the flexibility of the two-step scheme (9), in this subsection let us generate not only the existing FBP, backprojection filtration (BPF), backprojection (BP) and Λ reconstruction formulae, but also two new formulae by specifying suitable weight functions.

1) Weight function i: $w_S^i(\vec{k}) = w_S^i(\omega_1\vec{e}_1) = A_S$, where A_S denotes a real number dependent on the source position so that the weight function $w_S^i(\vec{k})$ is normalized, i.e., $w^i(\vec{k}) = \sum_{j=1}^{J_{\vec{k}}} A_{S^j} = 1$.

The filtered projection in Eq. (10) can be written as

$$\begin{aligned}\tilde{P}_S^i(t) &= \frac{A_S}{2\pi}\int_{-\infty}^{\infty} \exp(2\pi i\omega_1 t)\widehat{P}_S(\omega_1)(2\pi i\omega_1)(-isgn(\omega_1))d\omega_1 \\ &= \frac{A_S}{2\pi}\frac{d}{dt}(P_S(t) * \frac{1}{\pi t})\end{aligned}$$

where * denote the 1D convolution operator.

From Eq. (8) or Eq. (9), one arrives at the following reconstruction formula

$$\Psi(\vec{r}) = \Phi^i(\vec{r}) = \frac{1}{2\pi}\int_\Gamma A_S\frac{d}{dt}(P_S(t) * \frac{1}{\pi t})|d\theta| \tag{11}$$

If Γ is a 180° scan ($A_S = 1$), one obtain the standard FBP formula for parallel-beam CT

$$\Psi(\vec{r}) = \frac{1}{2\pi}\int_0^\pi \frac{d}{dt}(P_\theta(t) * \frac{1}{\pi t})d\theta.$$

2) Weight function ii: $w_S^{ii}(\vec{k}) = w_S^{ii}(\omega_1\vec{e}_1) = iA_S\text{sgn}(\omega_1)$, where the real number A_S satisfies $w^{ii}(\vec{k}) = \sum_{j=1}^{J_{\vec{k}}} A_{S^j}\text{sgn}(\omega_1) = i\text{sgn}(k_2)$.

The two-step formula (9) becomes the BPF formula for parallel-beam CT:

$$\Phi^{ii}(\vec{r}) = \frac{1}{2\pi}\int_\Gamma A_S\frac{d}{dt}P_S(t)|d\theta|$$

$$\widehat{\Phi}^{ii}(\vec{k}) = \widehat{\Psi}(\vec{k})i\text{sgn}(k_2)$$

$$\Psi(\vec{r}) = \Phi^{ii}(x,y) * \frac{1}{\pi y},$$

where the convolution is on the second variable y only.

If Γ is a 180° scan ($A_S = 1$), one has

$$\Phi^{ii}(\vec{r}) = \frac{1}{2\pi}\int_0^{\pi} \frac{d}{dt} P_\theta(t) d\theta.$$

3) Weight function iii: $w_S^{iii}(\vec{k}) = w_S^{iii}(\omega_1 \vec{e}_1) = \frac{A_S}{|\omega_1|}$ with $\sum_{j=1}^{J_{\vec{k}}} A_{S^j} = 1$.

The summed weight function $w^{iii}(\vec{k}) = \sum_{j=1}^{J_{\vec{k}}} \frac{A_{S^j}}{|\omega_1|} = \frac{1}{|\vec{k}|}\sum_{j=1}^{J_{\vec{k}}} A_{S^j} = \frac{1}{|\vec{k}|}$.

The two-step formula (9) becomes the BP formula for parallel-beam CT.

$$\Phi^{iii}(\vec{r}) = \int_\Gamma A_S P_S(t) |d\theta|$$

$$\widehat{\Phi}^{iii}(\vec{k}) = \widehat{\Psi}(\vec{k}) \frac{1}{|\vec{k}|}$$

$$\Psi(\vec{r}) = \Phi^{iii}(x, y) ** \frac{-1}{4\pi^2 |\vec{r}|^3}.$$

For a 180° scan and $A_S = 1$, one has

$$\Phi^{iii}(\vec{r}) = \int_0^{\pi} P_S(t) d\theta.$$

4) Weight function iv: $w_S^{iv}(\vec{k}) = w_S^{iv}(\omega_1 \vec{e}_1) = A_S |\omega_1|$ with $\sum_{j=1}^{J_{\vec{k}}} A_{S^j} = 1$.

The summed weight function is $w^{iv}(\vec{k}) = \sum_{j=1}^{J_{\vec{k}}} A_{S^j} |\omega_1| = |\vec{k}|$.

The two-step formula (9) becomes the Λ reconstruction formula

$$\Phi^{iv}(\vec{r}) = -\frac{1}{4\pi^2}\int_\Gamma A_S \frac{d^2}{dt^2} P_S(t) |d\theta|$$

$$\widehat{\Phi}^{iv}(\vec{k}) = \widehat{\Psi}(\vec{k}) |\vec{k}|$$

$$\Psi(\vec{r}) = \Phi^{iv}(\vec{r}) ** \frac{1}{|\vec{r}|}.$$

For a 180° scan and $A_S = 1$, one has

$$\Phi^{iv}(\vec{r}) = -\frac{1}{4\pi^2}\int_0^{\pi} \frac{d^2}{dt^2} P_S(t) d\theta.$$

5) Weight function v: $w_S^{v}(\vec{k}) = w_S^{v}(\omega_1 \vec{e}_1) = \frac{A_S}{|\omega_1 \sin\theta|}$, with $\sum_{j=1}^{J_{\vec{k}}} A_{S^j} = 1$.

The summed weight function is $w^v(\vec{k}) = \sum_{j=1}^{J_{\vec{k}}} \frac{A_{Sj}}{|\omega_1 \sin\theta|} = \frac{1}{|k_2|}$.

The two-step formula (9) becomes a new weighted backprojection (WBP) formula

$$\Phi^v(\vec{r}) = \int_\Gamma A_S P_S(t) \frac{1}{|\sin\theta|} |d\theta|$$

$$\widehat{\Phi}^v(\vec{k}) = \widehat{\Psi}(\vec{k}) \frac{1}{|k_2|}$$

$$\Psi(\vec{r}) = \Phi^v(x,y) * \frac{-1}{2\pi^2 y^2} = \left(\frac{\partial}{\partial y}\Phi^v(x,y)\right) * \frac{1}{2\pi^2 y}.$$

where the convolution * is applied on the second variable y.

For a 180° scan, taking $A_S = 1$ one has

$$\Phi^v(\vec{r}) = \int_0^\pi P_\theta(t) \frac{1}{|\sin\theta|} d\theta.$$

For a compactly supported function $\Psi(\vec{r})$, after $\Phi^v(\vec{r})$ is calculated one can calculate derivatives first and then reconstruct the object function via the finite inverse Hilbert transform [24]. As compared to the traditional BP algorithm, the advantage of the WBP algorithm lies in that the second step can be implemented line by line.

6) Weight function vi: $w_S^{vi}(\vec{k}) = w_S^{vi}(\omega_1 \vec{e}_1) = \frac{-iA_S}{\omega_1 \sin\theta}$, with $\sum_{j=1}^{J_{\vec{k}}} A_{Sj} = 1$.

The summed weight function is $w^{vi}(\vec{k}) = \sum_{j=1}^{J_{\vec{k}}} \frac{-iA_{Sj}}{\omega_1 \sin\theta} = \frac{-i}{k_2}$.

The two-step formula (9) becomes

$$\Phi^{vi}(\vec{r}) = \int_\Gamma A_S P_S(t) * \frac{1}{\pi t} \frac{1}{\sin\theta} |d\theta|$$

$$\widehat{\Phi}^{vi}(\vec{k}) = \widehat{\Psi}(\vec{k}) \frac{-i}{k_2}$$

$$\Psi(\vec{r}) = \frac{1}{2\pi}\left(\frac{\partial}{\partial y}\Phi^{vi}(x,y)\right).$$

For a 180° scan, taking $A_S = 1$ one has

$$\Phi^{vi}(\vec{r}) = \int_0^\pi P_\theta(t) * \frac{1}{\pi t} \frac{1}{\sin\theta} d\theta.$$

We temporarily call this formula the weighted Hilbert transform (WHT) method. As compared to the BPF algorithm, the order of the derivative operation and Hilbert transform is reversed. That is to say, in WHT we take the derivative of the intermediate image, instead of the projection dataset.

The FBP [2,22] and BPF [24] are well-known exact algorithms. The BP algorithm [3] and Λ reconstruction [4] are well-known approximate algorithm. The reconstruction from a BP intermediate function $\Phi^{iii}(\vec{r})$ to the object function $\Psi(\vec{r})$ was also studied [3,28]. To show the fertility of the two-step

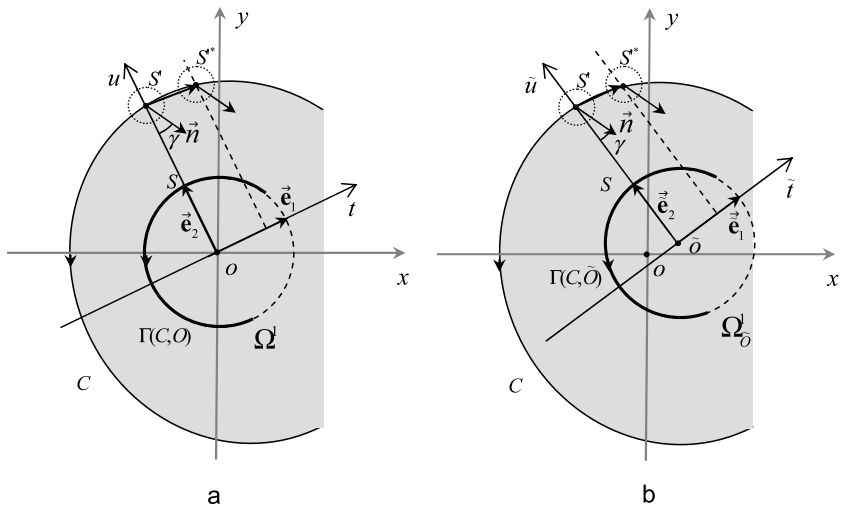

Fig. 4. Fan-beam reconstruction geometries for points O (a) and $\tilde{O}$ (b) respectively. The complete region of the scanning trajectory is shaded in gray.

scheme, we have introduced the two new algorithms: WBP and WHT. Detailed comparison of image quality and noise performance between the new and existing algorithms will be presented in a separate paper.

3. Fan-beam reconstruction

The fan-beam reconstruction is to calculate the function $\Psi(\vec{r})$ from its fan-beam projections, either exactly or approximately. In Fan-bean CT, a locus C consists of one or several continuous curves in the 2D space R^2, as shown in Fig. 4.

The fan-beam projection of the object function $\Psi(\vec{r})$ with respect to the locus C is defined as

$$p_{S'}(\vec{n}) = \int_0^\infty \Psi(\overrightarrow{OS'} + \vec{n}l)dl \tag{12}$$

for every $S' \in C$ and every unit vector $\vec{n} \in \Omega^1$.

The two elementary relations [22,29,30] between the parallel- and fan-beam projections are shown in Fig. 5, which will serve as the bridge between divergent and parallel-beam reconstructions.

In the 2D space R^2, a unit circle centered at a point $\tilde{O}$ is defined as

$$\Omega^1_{\tilde{O}} = \left\{ S : \overrightarrow{\tilde{O}S} = \vec{\tilde{e}}_2 = (-\sin\theta, \cos\theta), \theta \in [0, 2\pi) \right\}.$$

For a point $\tilde{O} \notin C$, the projection of the locus C on the unit circle $\Omega^1_{\tilde{O}}$ is defined as

$$\Gamma(C, \tilde{O}) = \left\{ S \in \Omega^1_{\tilde{O}} : \overrightarrow{\tilde{O}S} = \overrightarrow{\tilde{O}S'}/|\overrightarrow{\tilde{O}S'}|, S' \in C \right\}.$$

If $\Gamma(C, \tilde{O})$ is complete on the unit circle $\Omega^1_{\tilde{O}}$, we say that the trajectory C is complete with respect to $\tilde{O}$, or that $\tilde{O}$ is a complete point of the locus C. In the 2D space, the integrals along all the lines through a

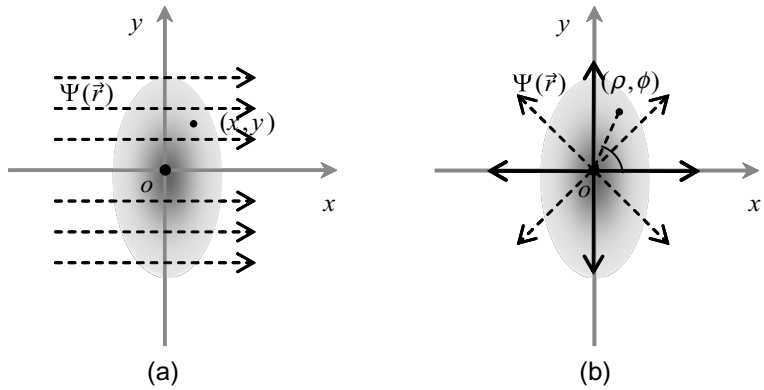

Fig. 5. Two basic relations between parallel- and fan-beam projections: $\iint_{R^2} \frac{1}{y}\Psi(x,y)dxdy = \int_{-\infty}^{\infty} \frac{1}{y} \int_{-\infty}^{\infty} \Psi(x,y)dxdy = \int_0^{2\pi} \frac{1}{\sin\phi} \int_0^{\infty} \Psi(\rho,\phi)d\rho d\phi$, $\int_{-\infty}^{\infty} \Psi(x,0)dx = \int_{-\infty}^{0} \Psi(x,0)dx + \int_0^{\infty} \Psi(x,0)dx$.

complete point are known. The set of the complete points is called the complete Region of the locus C, denoted as R(C), as shown in Fig. 4.

Our general conclusion on the fan-beam reconstruction goes as follows. For any point $\vec{r}$ in the complete region R(C), the value of the intermediate functions $\Phi^i(\vec{r}), \Phi^{ii}(\vec{r}), \Phi^{iii}(\vec{r}), \Phi^{iv}(\vec{r}), \Phi^{v}(\vec{r}), \Phi^{vi}(\vec{r})$, defined in the above section, can be calculated from fan-beam projection as well. This is due to the two relations between parallel- and fan-beam projections. Since $\Phi^i(\vec{r}) = \Psi(\vec{r})$, the complete region can be reconstructed from the fan-beam projections.

In order to translate the parallel-beam formulae to the divergent-beam case, let us exemplify a three-step method with the well-known FBP formula [22]. This framework will be used to obtain all the other divergent-beam formulae.

Step 1. Formulate the parallel-beam reconstruction at the origin O.

In Fig. 4a, we suppose that the origin O is a complete point of the locus C, i.e., $O \in R(C)$ and hence the projection of the locus C, $\Gamma(C,O)$, is a complete curve on the unit circle. We **assume** that there exists the parallel projection $P_S(t)$ for every $S \in \Gamma(C,O)$. For a given point $S \in \Gamma(C,O)$, the local coordinate system Otu is defined by the origin O and two unit vectors $\vec{e}_2 = \overrightarrow{OS}$ and $\vec{e}_1$ (obtained via rotating $\vec{e}_2$ clockwise by 90°), as we did in the above parallel-beam case.

Based on Eq. (11), the value of the object function at the origin can be calculate as follows

$$\begin{aligned}\Psi(O) = \Phi^i(O) &= \frac{1}{2\pi} \int_{\Gamma(C,O)} A_S \left.\frac{d}{dt}\right|_{t=0} (P_S(t) * \frac{1}{\pi t})|d\theta| \\ &= \frac{-1}{2\pi^2} \int_{\Gamma(C,O)} A_S \left.\frac{d}{dt}\right|_{t=0} \int_{-\infty}^{\infty} P_S(t+t')\frac{1}{t'}dt'|d\theta|.\end{aligned}$$

Step 2. Replace the parallel-beam projection by the fan-beam projection.

Please see Fig. 4a. Recall that S' is the intersection point between the half straight line OS and the locus C, i.e., $\overrightarrow{OS'}/|\overrightarrow{OS'}| = \overrightarrow{OS} = \vec{e}_2$. $S'^* \in C$ is another point on the locus beside S', whose local coordinates in the system Otu are $S'^*(t,u)$:

$$t = \overrightarrow{S'S'^*} \cdot \vec{e}_1 = \overrightarrow{OS'^*} \cdot \vec{e}_1, u = \overrightarrow{OS'^*} \cdot \vec{e}_2.$$

When $t = 0$, the point S'^* coincides the point S'.

As shown in Fig. 5, we have the following relations between the parallel-beam projection $P_S(t)$, and the fan-beam projection $p_{S'^*}(\vec{n})$, $\vec{n} \in \Omega^1$,

$$\int_{-\infty}^{\infty} P_S(t+t')\frac{1}{t'}dt' = \int_{-\pi}^{\pi} p_{S'^*(t,u)}(-\vec{e}_2\cos\gamma + \vec{e}_1\sin\gamma)\frac{1}{\sin\gamma}d\gamma$$
$$P_S(t) = p_{S'^*(t,u)}(-\vec{e}_2) + p_{S'^*(t,u)}(\vec{e}_2).$$

Therefore, the fan-bean reconstruction formula for the origin is

$$\Psi(O) = \frac{-1}{2\pi^2}\int_{\Gamma(C,O)} A_S \left.\frac{d}{dt}\right|_{t=0}\int_{-\pi}^{\pi} p_{S'^*(t,u)}(-\vec{e}_2\cos\gamma + \vec{e}_1\sin\gamma)\frac{1}{\sin\gamma}d\gamma|d\theta|,$$

where the derivative operation is implemented as

$$\left.\frac{d}{dt}\right|_{t=0}\int_{-\pi}^{\pi} p_{S'^*(t,u)}(-\vec{e}_2\cos\gamma + \vec{e}_1\sin\gamma)\frac{d\gamma}{\sin\gamma}$$
$$= \lim_{S'^*\to S'}\frac{1}{\overrightarrow{S'S'^*}\cdot\vec{e}_1}\int_{-\pi}^{\pi}[p_{S'^*}(-\vec{e}_2\cos\gamma + \vec{e}_1\sin\gamma) - p_{S'}(-\vec{e}_2\cos\gamma + \vec{e}_1\sin\gamma)]\frac{d\gamma}{\sin\gamma},$$

and A_S is dependent on $\Gamma(C, O)$.

Step 3. Translate the fan-beam formula to an arbitrary point $\tilde{O} \in R(C)$.

See Fig. 4b. Treating any complete point $\tilde{O} \in R(C)$ as a new origin point, we have

$$\Psi(\tilde{O}) = \frac{-1}{2\pi^2}\int_{\Gamma(C,\tilde{O})} A_S \left.\frac{d}{d\tilde{t}}\right|_{\tilde{t}=0}\int_{-\pi}^{\pi} p_{S'^*(\tilde{t},\tilde{u})}(-\vec{\tilde{e}}_2\cos\gamma + \vec{\tilde{e}}_1\sin\gamma)\frac{1}{\sin\gamma}d\gamma|d\theta|,$$

where S goes along $\Gamma(C, \tilde{O})$, and A_S is dependent on $\Gamma(C, \tilde{O})$.

Similarly, the derivative operation is implemented as

$$\left.\frac{d}{d\tilde{t}}\right|_{\tilde{t}=0}\int_{-\pi}^{\pi} p_{S'^*(\tilde{t},\tilde{u})}(-\vec{\tilde{e}}_2\cos\gamma + \vec{\tilde{e}}_1\sin\gamma)\frac{d\gamma}{\sin\gamma}$$
$$= \lim_{S'^*\to S'}\frac{1}{\overrightarrow{S'S'^*}\cdot\vec{\tilde{e}}_1}\int_{-\pi}^{\pi}\left[p_{S'^*}(-\vec{\tilde{e}}_2\cos\gamma + \vec{\tilde{e}}_1\sin\gamma) - p_{S'}(-\vec{\tilde{e}}_2\cos\gamma + \vec{\tilde{e}}_1\sin\gamma)\right]\frac{d\gamma}{\sin\gamma}.$$

The local coordinate system $\tilde{O}\tilde{t}\tilde{u}$ is determined by the origin $\tilde{O}$ and two unit vectors $\vec{\tilde{e}}_2 = \overrightarrow{\tilde{O}S}$ and $\vec{\tilde{e}}_1$ (obtained via rotating $\vec{\tilde{e}}_2$ clockwise by 90°). For example, the coordinates of the source position $S'^* \in C$ are

$$\tilde{t} = \overrightarrow{\tilde{O}S'^*}\cdot\vec{\tilde{e}}_1 = \overrightarrow{S'S'^*}\cdot\vec{\tilde{e}}_1, \tilde{u} = \overrightarrow{\tilde{O}S'^*}\cdot\vec{\tilde{e}}_2$$

In other words, the form of the formula has no change except that the point O is replaced by $\tilde{O}$. We use the notations $\vec{r} = \overrightarrow{O\tilde{O}}$, and $\Psi(\vec{r}) = \Psi(\tilde{O})$.

Repeating the above three steps, we have the following explicit formulae for the other five intermediate functions:

$$\Phi^{ii}(\tilde{O}) = \frac{1}{2\pi}\int_{\Gamma(C,\tilde{O})} A_S \left.\frac{d}{d\tilde{t}}\right|_{\tilde{t}=0} \left(p_{S'^*(\tilde{t},\tilde{u})}(\vec{\tilde{e}}_2) + p_{S'^*(\tilde{t},\tilde{u})}(-\vec{\tilde{e}}_2)\right)|d\theta|$$

$$\Phi^{iii}(\tilde{O}) = \int_{\Gamma(C,\tilde{O})} A_S \left(p_{S'}(\vec{\tilde{e}}_2) + p_{S'}(-\vec{\tilde{e}}_2)\right)|d\theta|$$

$$\Phi^{iv}(\tilde{O}) = -\frac{1}{4\pi^2}\int_{\Gamma(C,\tilde{O})} A_S \left.\frac{d^2}{d\tilde{t}^2}\right|_{\tilde{t}=0} \left(p_{S'^*(\tilde{t},\tilde{u})}(\vec{\tilde{e}}_2) + p_{S'^*(\tilde{t},\tilde{u})}(-\vec{\tilde{e}}_2)\right)|d\theta|$$

$$\Phi^{v}(\tilde{O}) = \int_{\Gamma(C,\tilde{O})} \frac{A_S}{|\sin\theta|}\left(p_{S'}(\vec{\tilde{e}}_2) + p_{S'}(-\vec{\tilde{e}}_2)\right)|d\theta|$$

$$\Phi^{vi}(\tilde{O}) = -\frac{1}{\pi}\int_{\Gamma(C,\tilde{O})} \frac{A_S}{\sin\theta}\int_{-\pi}^{\pi} p_{S'}(-\vec{\tilde{e}}_2\cos\gamma + \vec{\tilde{e}}_1\sin\gamma)\frac{1}{\sin\gamma}d\gamma|d\theta|.$$

After the value of the intermediate function has been calculated in the complete region of a locus, the next step is the same as in the parallel-beam case. One can either use the intermediate functions for an approximate reconstruction or exactly reconstruct the object function from them. They allow the FBP [22,23], BPF [24], BP [3], Λ reconstruction [4,31,32], new WBP and WHT for image reconstruction from fan-beam data.

Note that the above lambda reconstruction formula, $\Phi^{iv}(\tilde{O})$, is based on the even extension of the projection data. However, in our former paper [31] we claimed that the lambda reconstruction can be based on either the even or odd extension. Now, we realize that in [31] Formula (9) based on the odd extension is not generally correct, because Eq. (31) must hold on the whole plane instead of at only one point x_0 to obtain Eq. (32). Therefore, Theorem 1 in [31] does not hold generally. As a fix, the correct result has appeared in our new paper [32].

4. 3D parallel-beam reconstruction

4.1. Inverse Fourier transform in different coordinate systems

In the 3D space R^3, $\Psi(\vec{r})$ is an object function to be reconstructed whose Fourier transform is $\widehat{\Psi}(\vec{k})$. According to Fourier analysis, we have

$$\Psi(\vec{r}) = \int_{-\infty}^{\infty}\int_{-\infty}^{\infty}\int_{-\infty}^{\infty} \widehat{\Psi}(\vec{k})\exp(2\pi i\vec{k}\cdot\vec{r})dk_1dk_2dk_3$$

where $\vec{r} = (x, y, z)$ and $\vec{k} = (k_1, k_2, k_3)$ are 3D vectors in the real space and Fourier domain, respectively. In the spherical and cylindrical coordinate systems, the inverse Fourier transform is expressed as

$$\Psi(\vec{r}) = \int_0^{2\pi}\int_0^{\pi}\int_0^{\infty} \widehat{\Psi}(\vec{k})\exp(2\pi i\vec{k}\cdot\vec{r})k^2dk\sin\theta d\theta d\phi \tag{a}$$

$$= \int_0^{\pi}\int_0^{\pi}\int_{-\infty}^{\infty} \widehat{\Psi}(\vec{k})\exp(2\pi i\vec{k}\cdot\vec{r})k^2dk\sin\theta d\theta d\phi \tag{b}$$

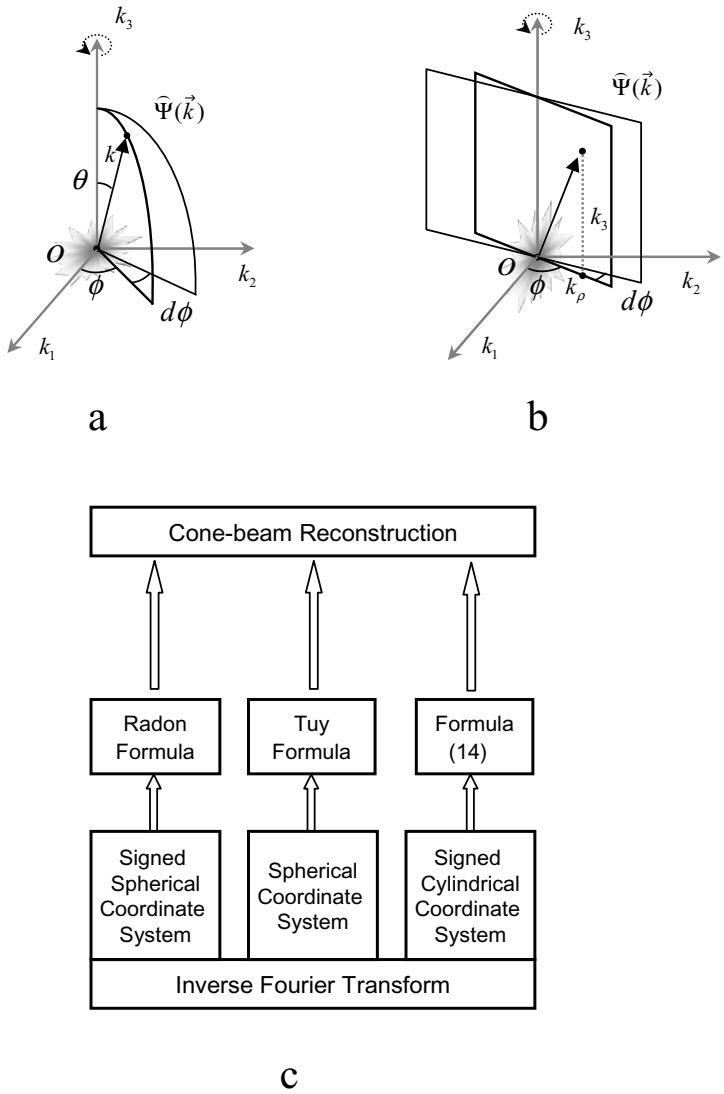

Fig. 6. Different coordinate systems for the inverse Fourier transform. The spherical (a) and cylindrical (b) coordinate systems for the inverse Fourier transform lead to different schemes for cone-beam reconstruction (c).

$$= \int_0^{\pi} \int_{-\infty}^{\infty} \int_{-\infty}^{\infty} \widehat{\Psi}(\vec{k}) \exp(2\pi i \vec{k} \cdot \vec{r}) |k_\rho|_d k_\rho dk_3 d\phi \tag{c}$$

as shown in Fig. 6.

In Formula (a), the standard spherical coordinate (k, θ, ϕ) is used with $0 \leqslant k < \infty, 0 \leqslant \theta \leqslant \pi, 0 \leqslant \phi < 2\pi$, while in Formula (b) a signed spherical coordinate (k, θ, ϕ) is used with $-\infty < k < \infty,\ 0 \leqslant \theta \leqslant \pi,\ 0 \leqslant \phi < \pi$. Historically, Tuy started with (a) to develop a fundamental formula for cone-beam

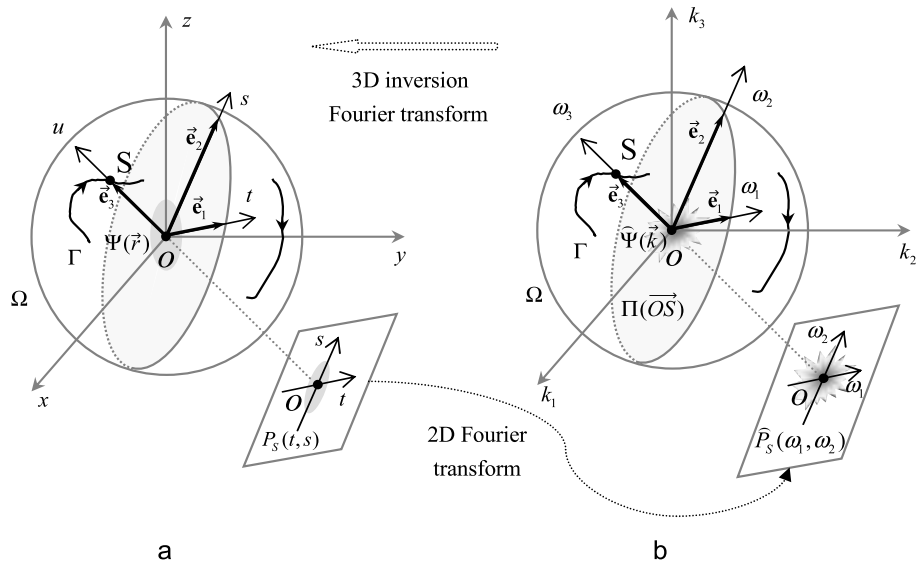

Fig. 7. 3D parallel-beam reconstruction geometry. (a) A projection plane in the real space, and (b) a frequency plane in the Fourier space.

CT [27], and the classic Radon formula

$$\Psi(\vec{r}) = -\frac{1}{4\pi^2}\int_0^{\pi}\int_0^{\pi}\frac{\partial^2}{\partial l^2}Rf(l,\theta,\phi)\,\big|_{l=\vec{r}\cdot(\sin\theta\cos\phi,\sin\theta\sin\phi,\cos\theta)}\,\sin\theta d\theta d\phi,$$

can be obtained from (b) easily though Radon discovered his formula in another way [5]. This is a reason why we have two different schemes [15,21,23,26] in the CT field. In Formula (c), the signed cylindrical coordinate (k_ρ, k_3, ϕ) with $-\infty < k_\rho < \infty, -\infty < k_3 < \infty, 0 \leqslant \phi < \pi$ is used. Our discussion will start from an improved form of Formula (c), which proves to be convenient for both parallel- and cone-beam reconstruction [12,28] and, more importantly, make the 3D reconstruction problems very similar to the 2D counterparts. This is the elementary difference between our scheme and the existing ones.

In (c), when ϕ increase from 0 to π, the plane $Ok_\rho k_3$ scans every point in the frequency space once and only once (Fig. 6b). We will keep this observation in mind when we deal with more complicated cases. Two related concepts we will use are the complete curve and weight function.

4.2. Complete curves on the unit sphere

As shown in Fig. 7, in the 3D space R^3, $\Psi(\vec{r})$ represents the object to be reconstructed, whose Fourier transform is denoted by $\widehat{\Psi}(\vec{k})$.

The end points of all the unit vectors form the unit sphere in the space R^3

$$\Omega = \left\{ S \in R^3 : |\overrightarrow{OS}| = |\vec{e}_3| = 1 \right\}. \tag{13}$$

A curve Γ on the unit sphere Ω consists of a number of differentiable segments, each of which has the tangential direction at every point. Γ is called complete on Ω if it intersects every great circle of

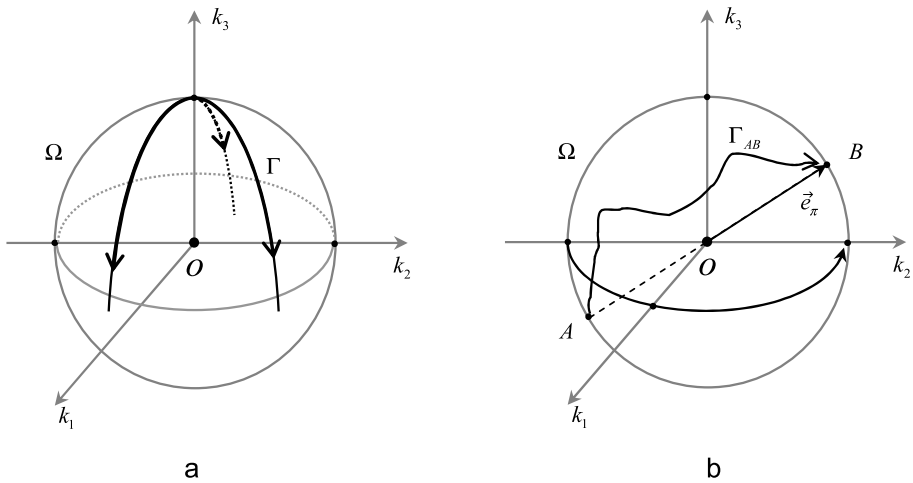

Fig. 8. Completeness of curves on the unit sphere. (a) Three symmetrical arcs starting from the point (0, 0,1) are extended downward. Before they pass the horizontal equator, they are incomplete (thick lines); then, they become complete (thin lines); and (b) any continuous and piecewise differentiable trace Γ_{AB} from A to its opposite point B is a simple complete curve, with the simplest complete curve being half a great circle.

Ω [33,34]. Clearly, half a great circle is the simplest complete curve. Another simple complete curve is a continuous and piece-wise differentiable curve connecting two endpoints of a diameter AB of Ω, denoted by Γ_{AB} (Fig. 8). Again, in this paper all the formulae are based on complete curves unless otherwise stated.

For a point S on the unit sphere in the frequency space, the plane through the origin O and orthogonal to the normal vector $\overrightarrow{OS} = \vec{e}_3$

$$\Pi(\overrightarrow{OS}) = \left\{ \vec{k} \in R^3 : \vec{k} \cdot \overrightarrow{OS} = 0 \right\}$$

is called a frequency plane (Fig. 7b). When the point S moves along a complete curve Γ, the frequency plane $\Pi(\overrightarrow{OS})$ scans the entire frequency space. When the point S moves along a complete curve Γ, the times the plane $\Pi(\overrightarrow{OS})$ passes a given point $\vec{k}$ can be viewed as a function defined in the Fourier domain $J(\vec{k})$, or $J_{\vec{k}}$, satisfying that $J(c\vec{k}) = J(\vec{k})$ for any real number $c \neq 0$. Geometrically speaking, the great circle orthogonal to the vector $\vec{k}$ intersects the curve Γ at $J(\vec{k})$ points, denoted as $S^j, j = 1, 2, \ldots, J(\vec{k})$. For a complete curve, $J(\vec{k}) \geqslant 1$ everywhere. For half a great circle, we have $J(\vec{k}) = 1$ over the entire space. A concrete complete curve and its $J(\vec{k})$ function are given in Fig. 9.

4.3. The 3D version of the two-step formula for parallel-beam problem

As shown in Fig. 7, for every point $S \in \Gamma$, we define a local coordinate system in terms of three unit vectors $\vec{e}_3 = \overrightarrow{OS}, \vec{e}_1$ following the tangential direction of Γ at S, and $\vec{e}_2 = \vec{e}_3 \times \vec{e}_1$. The space vectors and frequency vector have the following components respectively:

$$t = \vec{r} \cdot \vec{e}_1, s = \vec{r} \cdot \vec{e}_2, u = \vec{r} \cdot \vec{e}_3;$$
$$\omega_1 = \vec{k} \cdot \vec{e}_1, \omega_2 = \vec{k} \cdot \vec{e}_2, \omega_3 = \vec{k} \cdot \vec{e}_3.$$

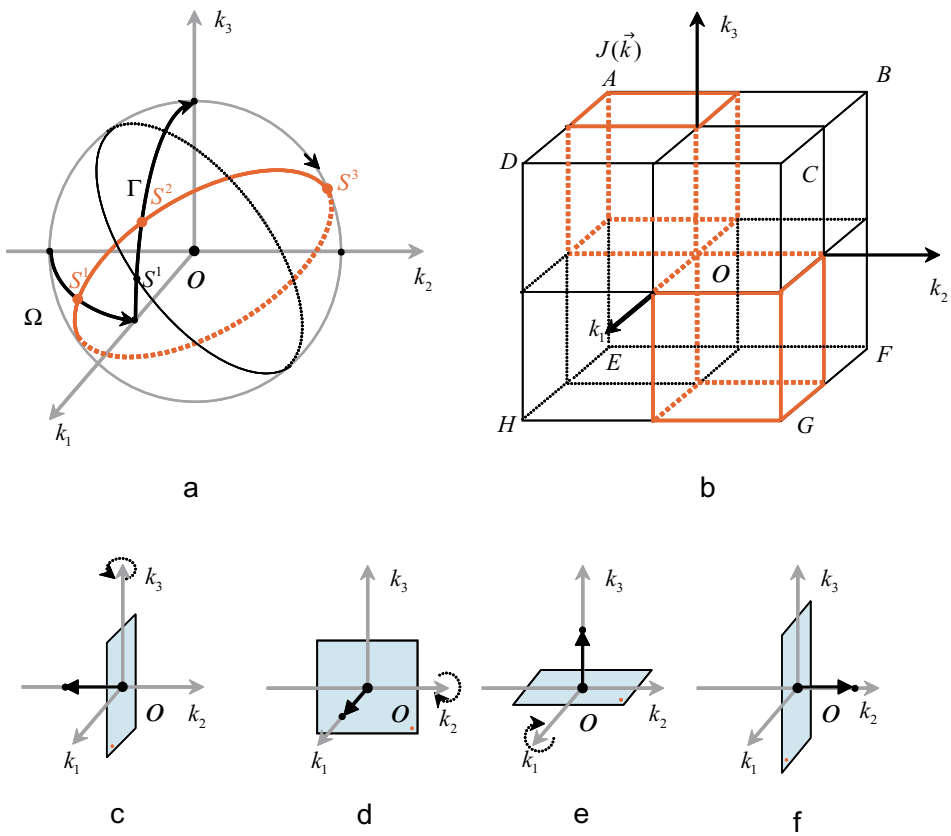

Fig. 9. A complete curve and its J(k) function. (a) A curve consisting of three orthogonal quarter great circles, i.e., the trajectory when a point is moved along the path (0, −1, 0) → (1, 0, 0) → (0, 0, 1) → (0, 1, 0), (b) J(k) is equal to 3 inside the two regions marked by the red lines and 1 elsewhere, and (c)–(f) four representative positions of the frequency plane.

The parallel-beam projection along $\overrightarrow{OS}$ is defined as

$$P_S(t,s) = \int_{-\infty}^{\infty} \Psi(t\vec{e}_1 + s\vec{e}_2 + u\vec{e}_3)du,$$

whose Fourier transform is

$$\widehat{P}_S(\omega_1,\omega_2) = \int_{R^2} P_S(t,s)\exp[-2\pi i(\omega_1 t + \omega_2 s)]dtds.$$

In the real space R^3, the plane Ots is called a projection plane (Fig. 7a).

The Fourier transform of the projection and the object are related by Fourier slice theorem

$$\widehat{P}_S(\omega_1,\omega_2) = \widehat{\Psi}(\vec{k})\Big|_{\vec{k}=\omega_1\vec{e}_1+\omega_2\vec{e}_2}.$$

If the projection $P_S(t,s)$ is known for all points S on a complete curve Γ, the object function $\Psi(\vec{r})$ can be recovered from its Fourier transform $\widehat{\Psi}(\vec{k})$:

$$\Psi(\vec{r}) = \int_{R^3} \widehat{\Psi}(\vec{k})\exp(2\pi i\vec{k}\cdot\vec{r})d\vec{k}^3$$

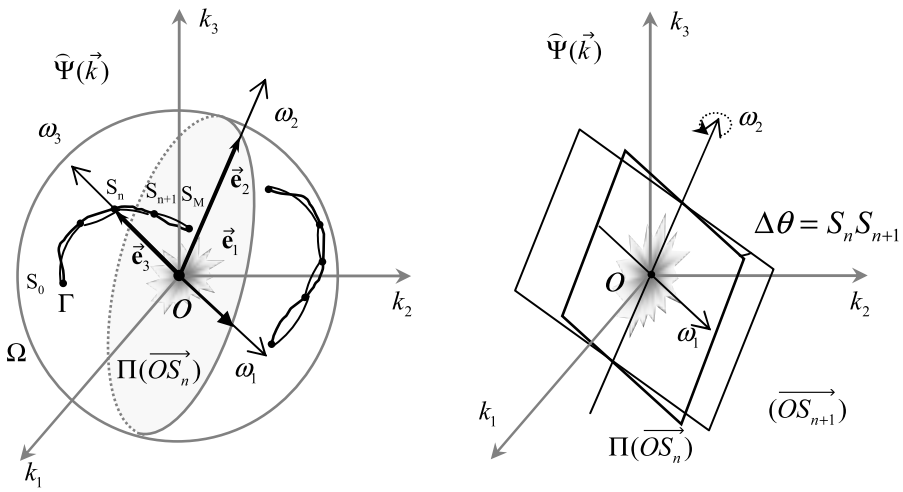

Fig. 10. When S moves along a continuous curved segment, the frequency plane moves continuously in the frequency space. The segment can be divided at M points and approximated as a series of great arcs, and the motion of the frequency plane can be approximated a series of small rotations. Here S_nS_{n+1} denotes the length of the great arc between the two points S_n and S_{n+1}. For simplicity, we further assume that the segment is differentiable.

$$= \int_\Gamma \int_{\Pi(\overrightarrow{OS})} \exp(2\pi i\vec{k}\cdot\vec{r})\widehat{P}_S(\omega_1,\omega_2)w_S(\vec{k})|\omega_1|d\omega_1 d\omega_2 d\theta \tag{14}$$

where $d\theta$ is the length of the differential arc along Γ. Different from 2D case, $d\theta$ is always positive here. For simplicity, the integration plane $\Pi(\overrightarrow{OS})$ is denoted by R^2 in the following. See Fig. 10 for more explanation on Formula (14).

The weight function $w_S(\vec{k})$ in Eq. (14), defined for every $S \in \Gamma$ and all $\vec{k} \in \Pi(\overrightarrow{OS})$, is used to handle the over-sampling of frequency components. Since a frequency point $\vec{k}$ is swept by the frequency plane $J_{\vec{k}}$ times, it is required that the summed weight function $\sum_{j=1}^{J_{\vec{k}}} w_{S^j}(\vec{k}) = 1$, where $S^j, j = 1, 2, \ldots, J_{\vec{k}}$ are the intersection points between the curve and the great circle orthogonal to the vector $\vec{k}$.

The reconstruction process based on Eq. (14) consists of the three steps: (1) calculate the Fourier transform of every measured projection $P_S(t,s)$, (2) weight the Fourier transform $\widehat{P}_S(\omega_1,\omega_2)$ by a weight function $w_S(\vec{k})|\omega_1|$, and (3) reconstruct the function $\Psi(\vec{r})$ via a 3D inversion Fourier transform (Fig. 7). To our best knowledge, it is the first time that this formula is explicitly given, which can be considered as an improved form of the inverse Fourier transform in the cylindrical coordinate system.

When an object can be fully covered by a parallel-beam, the reconstruction problem is solved by Eq. (14) or other equivalent formulae [28] such as the classical Radon's [5] or Orlov's formula [33,34]. For a long object, such as human body, it is impossible for an x-ray beam to cover the entire object. Therefore, a more practical problem is to reconstruct a part of the object from truncated projections ($p_S(t,s)$ known in a region of the projection plane Ots). This is called the long object problem of 3D CT [12,28].

To deal with various cases, let us generalize Eq. (14) into a more flexible two-step form. For a general weight function $w_{S^j}(\vec{k})$ whose summation is denoted as $\sum_{j=1}^{J_{\vec{k}}} w_{S^j}(\vec{k}) = w(\vec{k})$, we have

$$\Phi(\vec{r}) = \int_\Gamma \int_{R^2} \exp(2\pi i\vec{k}\cdot\vec{r})\widehat{P}_S(\omega_1,\omega_2)w_S(\vec{k})|\omega_1|d\omega_1 d\omega_2 d\theta,$$

$$\widehat{\Phi}(\vec{k}) = \widehat{\Psi}(\vec{k})w(\vec{k}), \tag{15}$$

where the function $\Phi(\vec{r})$ is called an intermediate function with the Fourier transform $\widehat{\Phi}(\vec{k})$. For a normalized weight function, whose summed weight function $w(\vec{k}) = 1$, the intermediate function $\Phi(\vec{r})$ is identical to the object, i.e., $\Phi(\vec{r}) = \Psi(\vec{r})$. Hence, Eq. (14) is a special case of Eq. (15). For a general weight function, the resultant intermediate function $\Phi(\vec{r})$ can be used as an approximation to the object function, or it can be based upon to reconstruct the object function $\Psi(\vec{r})$ via a second-step filtration if $w(\vec{k}) \neq 0$:

$$\widehat{\Psi}(\vec{k}) = \widehat{\Phi}(\vec{k})/w(\vec{k}). \tag{16}$$

For convenience, the inner integral in Eq. (15) is also called the filtered projection:

$$\begin{aligned}\tilde{P}_S(t,s) &= \int_{R^2} \exp(2\pi i(\omega_1 t + \omega_2 s)\widehat{P}_S(\omega_1,\omega_2)w_S(\vec{k})|\omega_1|d\omega_1 d\omega_2 \\ &= \frac{1}{2\pi}\frac{\partial}{\partial t}\int_{R^2} \exp(2\pi i(\omega_1 t + \omega_2 s)\widehat{P}_S(\omega_1,\omega_2)w_S(\vec{k})(-i)\mathrm{sgn}(\omega_1)d\omega_1 d\omega_2.\end{aligned} \tag{17}$$

4.4. Reconstruction formulae for 3D parallel-beam problem

Let us develop new reconstruction formulae suitable for truncated parallel-beam projections. Our method is to choose some special weight functions so that the filtered projection in Eq. (17) can be calculated from **a part of** projection on the plane Ots.

1) Weight function I: $w_S^I(\vec{k})$ (**Dartboard function**)

For any complete curve Γ, based on the definition, the function $J(\vec{k})$ has the symmetry

$$J(c\vec{k}) = J(\vec{k})$$

for any real number $c \neq 0$. Since the values of $J(\vec{k})$ are integers, it is reasonable to assume $J(\vec{k})$ is piecewise constant for a practical complete curve Γ. Therefore, we consider a piecewise constant weight function with the same symmetry, **dartboard** function.

Let (ρ, α) with $\rho \in [0, \infty), \alpha \in [-\pi/2, 3\pi/2)$ be the polar coordinates associated with the frequency point (ω_1, ω_2) in the frequency plane $\Pi(\overrightarrow{OS})$, the polar coordinate axis being $O\omega_1$. See Fig. 11. There are M+1 real numbers β_m with $-\pi/2 = \beta_0 < \beta_1 < \cdots < \beta_m < \cdots < \beta_M = \pi/2$. Furthermore, let $\alpha_m = \beta_m + \pi/2$.

Now for a source point S on a complete curve Γ, i.e., $S \in \Gamma$, we define the normal weight function $w_S^I(\vec{k})$ satisfying

$$\begin{aligned} &w_S^I(\rho,\alpha) = d_m, \beta_m < \alpha < \beta_{m+1}, m = 0, 1, \cdots, M-1 \\ &w_S^I(\rho, \alpha+\pi) = w_S^I(\rho,\alpha), \end{aligned} \tag{18}$$

where d_m, $m = 0, 1, 2, \ldots, M-1$, are M real numbers. Since the weight function defined in Eq. (18) looks like a dartboard marked with the same scores at opposite positions, we call it a dartboard function.

In the frequency plane $\Pi(\overrightarrow{OS})$, we denote a basic function as

$$h(\rho,\alpha) = h(\alpha) = \begin{cases} 1 & \alpha \in (-\pi/2, \pi/2) \\ -1 & \alpha \in (\pi/2, 3\pi/2) \end{cases}.$$

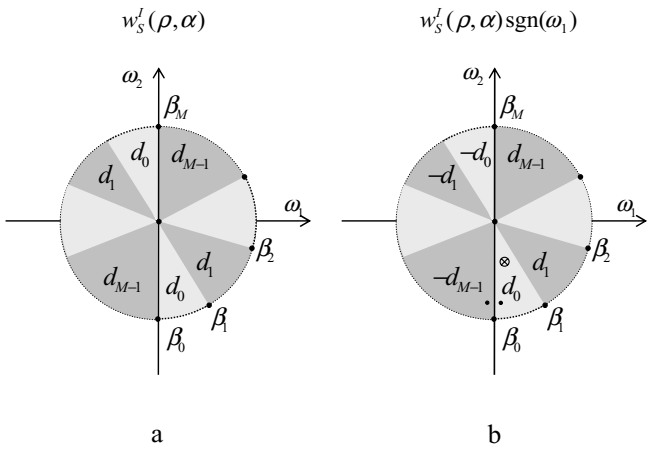

Fig. 11. (a) A dartboard function, and (b) the product of the Dartboard function and the sign function.

Proposition. The product of a dartboard function $w_S^I(\vec{k})$ and a sign function sgn(ω_1) can be uniquely decomposed as a summation of basic functions, i.e.,

$$\mathrm{sgn}(\omega_1)w_S^I(\omega_1,\omega_2) = \sum_{m=0}^{M-1} c_m h(\alpha-\alpha_m), \tag{19}$$

where

$$\begin{array}{l} c_0 = \frac{1}{2}(d_0+d_{M-1}) \\ c_m = \frac{1}{2}(d_m - d_{m-1}) \\ (m=1,2,3,\ldots,M-1) \end{array} .$$

Proof. First, it is easy to verify that the decomposition holds with the given $c_m, m=0,\ldots,M-1$.

For example, for the region $\beta_0<\alpha<\beta_1$, the two sides of Eq. (19) are identical:

$$\frac{1}{2}(d_0+d_{M-1}) - \frac{1}{2}(d_1-d_0) - \frac{1}{2}(d_2-d_1) - \ldots - \frac{1}{2}(d_{M-1}-d_{M-2}) = d_0.$$

Then, we can show that the coefficients $c_m, m=0,\ldots,M-1$, are unique. Suppose that there is another decomposition

$$\mathrm{sgn}(\omega_1)w_S^I(\omega_1,\omega_2) = \sum_{m=0}^{M-1} c'_m h(\alpha-\alpha_m).$$

Considering the difference between the two sides of $\alpha=-\pi/2$, we have

$$c'_0 = \frac{1}{2}(d_0+d_{M-1}) = c_0.$$

For the same reason, all the coefficients $c'_m = c_m,$ for $m=0,\ldots,M-1.$ This completes the proof.

Let the function $\widehat{f}_S^I(\omega_1,\omega_2) = (-i)\mathrm{sgn}(\omega_1)w_S^I(\vec{k})$ denote the filter in Eq. (17), and $f_S^I(t,s)$ denote its corresponding spatial function.

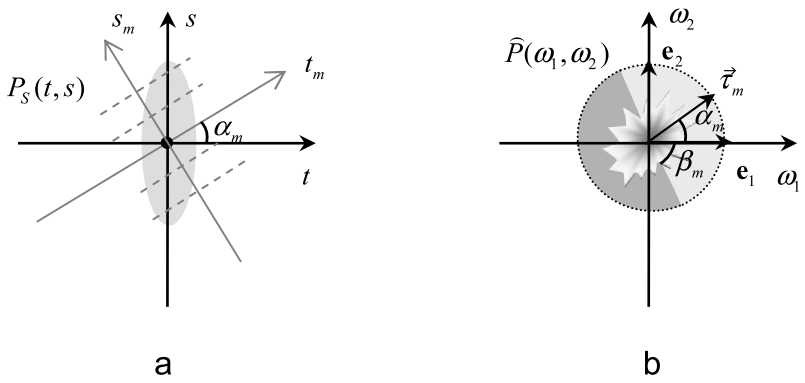

Fig. 12. By the convolution theorem, a convolution in the real space (a) is equivalent to a multiplication in the Fourier domain (b): $P_S(t,s) * 1/(\pi t_m) \Leftrightarrow -i\widehat{P}(\omega_1,\omega_2)h(\alpha-\alpha_m)$. Note that the 1D convolution can be done line by line. $\vec{\tau}_m$ is a unit vector defined by $\vec{\tau}_m = \vec{e}_1\cos\alpha_m + \vec{e}_2\sin\alpha_m$.

Due to the Proposition, the filter $\widehat{f}^I_S(\omega_1,\omega_2)$ can be uniquely decomposed into a sum of several Hilbert filters

$$\widehat{f}^I_S(\omega_1,\omega_2) = (-i)\sum_{m=0}^{M-1} c_m h(\alpha-\alpha_m),$$

where $(-i)\ h(\alpha-\alpha_m)$ is the m-th Hilbert filter.

Based on the theory of generalized functions [35], we have

$$\int_{R^2} -i\mathrm{sgn}(\omega_1)\exp(2\pi i(\omega_1 t+\omega_2 s))d\omega_1 d\omega_2 = \frac{1}{\pi t}\delta(s).$$

Therefore, the corresponding spatial function of the m-th Hilbert filter is given by

$$\int_{R^2} -ih(\alpha-\alpha_m)\exp(2\pi i(\omega_1 t+\omega_2 s))d\omega_1 d\omega_2 = \frac{1}{\pi t_m}\delta(s_m),$$

where $t_m = t\cos\alpha_m + s\sin\alpha_m$, $s_m = -t\sin\alpha_m + s\cos\alpha_m$ are the coordinates in a system rotated with an angle α_m. The m-th filter and its related convolution operation are shown in Fig. 12. The vector $\vec{\tau}_m = \vec{e}_1\cos\alpha_m + \vec{e}_2\sin\alpha_m$ is called m-th filtering direction.

Now, we obtain

$$\begin{aligned} f^I_S(t,s) &= \int_{R^2}\exp(2\pi i(\omega_1 t+\omega_2 s))(-i)\sum_{m=0}^{M-1} c_m h(\alpha-\alpha_m)d\omega_1 d\omega_2 \\ &= \sum_{m=0}^{M-1}\frac{c_m}{\pi t_m}\delta(s_m). \end{aligned} \tag{20}$$

Therefore, Eq. (17) can be written as

$$\tilde{P}^I_S(t,s) = \frac{1}{2\pi}\frac{\partial}{\partial t}\left(P_S(t,s) ** f^I_S(t,s)\right)$$

$$= \frac{1}{2\pi}\frac{\partial}{\partial t}\left(\sum_{m=0}^{M-1} c_m P_S(t,s) ** \frac{1}{\pi t_m}\delta(s_m)\right)$$

$$= \frac{1}{2\pi}\frac{\partial}{\partial t}\left(\sum_{m=0}^{M-1} c_m P_S(t,s) * \frac{1}{\pi t_m}\right)$$

$$= -\frac{1}{2\pi^2}\frac{\partial}{\partial t}\left(\sum_{m=0}^{M-1} c_m \int_{-\infty}^{\infty} P_S(t+t'\cos\alpha_m, s+t'\sin\alpha_m)\frac{1}{t'}dt'\right),$$

where the Dirac function turns the 2D convolution (**) into a 1D convolution (*), which can be implemented line by line. In the projection plane, to calculate the filtered projection at a given point (t, s), we use the projection data on several lines (including its neighborhood for the derivative operation) through the point (t, s) rather than projection data on the entire projection plane. Thus, the reconstruction formulae (14 or 15) actually allows those types of data truncations that do not interfere the required Hilbert filtering:

$$\Psi(\vec{r}) = \Phi^I(\vec{r}) = -\frac{1}{2\pi^2}\int_\Gamma \frac{\partial}{\partial t}\sum_{m=0}^{M-1} c_m \int_{-\infty}^{\infty} P_S(t+t'\cos\alpha_m, s+t'\sin\alpha_m)\frac{1}{t'}dt'd\theta. \tag{21}$$

For example, the value at the origin can be reconstructed by

$$\Psi(O) = -\frac{1}{2\pi^2}\int_\Gamma \left.\frac{\partial}{\partial t}\right|_{t=0}\sum_{m=0}^{M-1} c_m \int_{-\infty}^{\infty} P_S(t+t'\cos\alpha_m, t'\sin\alpha_m)\frac{1}{t'}dt'd\theta. \tag{22}$$

Figure 13 indicates a weight function ($M = 2$) and its associated filter, which is decomposed into two basic filters. The projection data used to calculate the filtered projection $\tilde{P}_S(0,0)$ is also marked.

Now, let us study the case of the simple complete curve. For a simple complete curve Γ_{AB} on the unit sphere (Fig. 14a), a weight function can be defined as

$$w_S^{I1}(\vec{k}) = \text{sgn}(\vec{k}\cdot\vec{e}_\pi)\text{sgn}(\vec{k}\cdot\vec{e}_1) = \text{sgn}(\vec{k}\cdot\vec{e}_\pi)\text{sgn}(\omega_1)$$

for all $\vec{k} \in \Pi(\overrightarrow{OS})$, where $\vec{e}_\pi = \overrightarrow{OB}$ is the unit vector from A and B. This weight function is normalized, i.e.,

$$\sum_{j=1}^{J_{\vec{k}}} \text{sgn}(\vec{k}\cdot\vec{e}_\pi)\text{sgn}(\omega_1) = \sum_{j=1}^{J_{\vec{k}}} \text{sgn}(\vec{k}\cdot\vec{e}_\pi)\text{sgn}(\vec{k}\cdot\vec{e}_1(S^j)) = 1 \tag{23}$$

for all $\vec{k} \in R^3$, where $\vec{e}_1(S^j)$ is the tangential direction of the curve Γ_{AB} at S^j, the j-th intersection point between Γ_{AB} and the unit circle orthogonal to $\vec{k}$.

A simple justification for that normality goes as follows. The weight function $w_S^{I1}(\vec{k})$ takes on the value of either 1 or -1, indicating the direction in which the frequency point passes through the frequency plane. Clearly, when the source point S moves from A to B, the frequency plane is turned over and every frequency point is swept once and only once if two passes in the opposite directions are not counted. In Fig. 14, we show the weight function and its filter. To explain the normality of this function in detail, an intuitive analogy is provided in Appendix A.

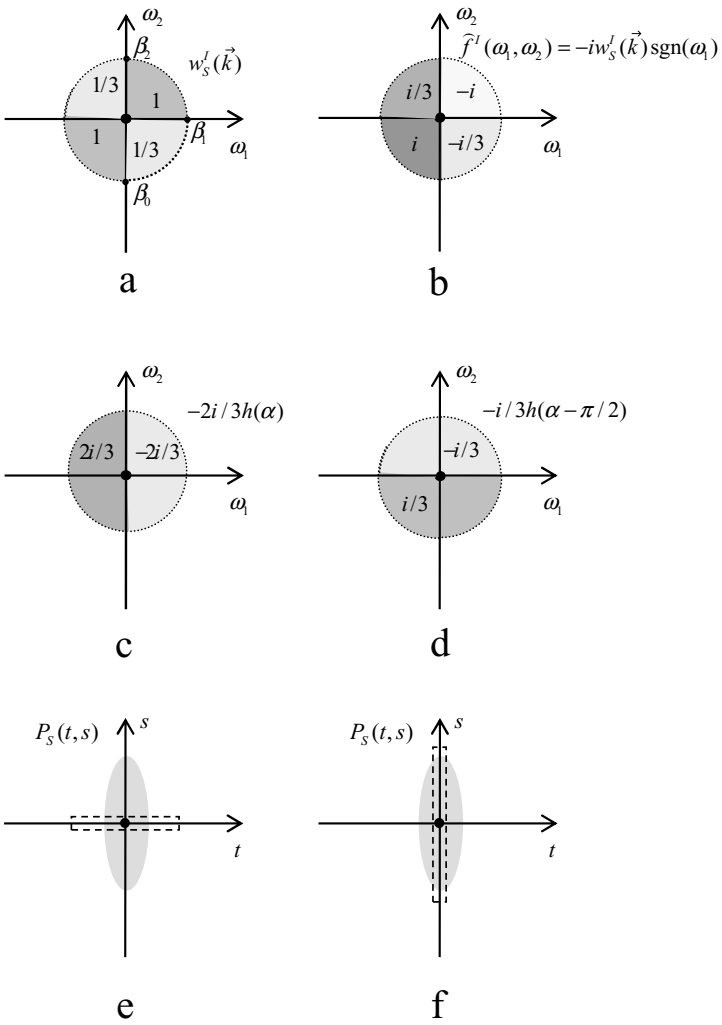

Fig. 13. Example of the dartboard function $w_S^I(\vec{k})$ and its decomposition. For a given weight function (a), its filter (b) can be decomposed into a sum of two basic filters (c) and (d): $\widehat{f}^I(\omega_1,\omega_2) = -iw_S^I(\vec{k})\mathrm{sgn}(\omega_1) = -2i/3h(\alpha) - i/3h(\alpha_\pi/2)$ with the spatial function $f^I(t,s) = \frac{2\delta(s)}{s\pi t} + \frac{\delta(t)}{3\pi s}$. For computation of the filtered projection at the origin, only the projection data indicated in (e) and (f) are involved.

Associated with the weight function $w_S^{I1}(\vec{k})$, the filter and the convolution kernel are

$$\widehat{f}_S^{I1}(\omega_1,\omega_2) = -i\mathrm{sgn}(\vec{k}\cdot\vec{e}_\pi) = -i\mathrm{sgn}(\vec{k}\cdot\vec{\tau}_1),$$

$$f_S^{I1}(t,s) = \frac{1}{\pi t_1}\delta(s_1),$$

and the filtered projection becomes

$$\tilde{P}_S^{I1}(t,s) = \frac{1}{2\pi}\frac{\partial}{\partial t}\left[P_S(t,s) * \frac{1}{\pi t_1}\right],$$

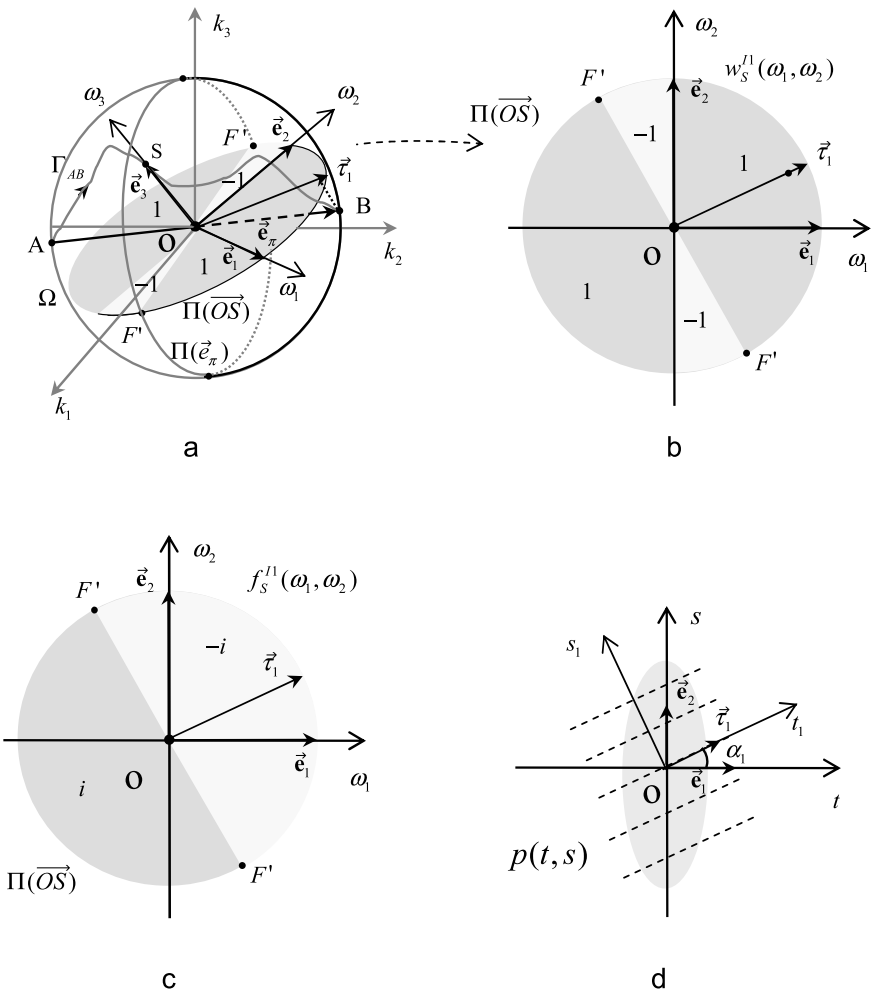

Fig. 14. Weight function $w_S^{I1}(\omega_1,\omega_2)$ and the filter related to the curve Γ_{AB}. In (a) and (b), Γ_{AB} is a curve connecting the two end points of the diameter AB and FF' is the intersection line between $\Pi(\vec{OS})$ and the plane orthogonal to $\vec{e}_\pi = \vec{OB}$, $\vec{\tau}_1$ the unit vector along the projection of the vector $\vec{\mathbf{e}}_\pi$ on the plane $\Pi(\vec{OS})$; (c) and (d) show the filter in the Fourier domain and the direction of the convolution in the real space, respectively.

where the unique filtering direction is along $\vec{\tau}_1$, which is the unit vector along the projection of $\vec{e}_\pi$ on the plane $\Pi(\overrightarrow{OS})$:

$$\vec{\tau}_1 = (\vec{e}_\pi - (\vec{e}_\pi \cdot \vec{e}_3)\vec{e}_\pi)/|\vec{e}_\pi - (\vec{e}_\pi \cdot \vec{e}_3)\vec{e}_\pi|.$$

The reconstruction formula (21) now becomes

$$\Psi(\vec{r}) = -\frac{1}{2\pi^2}\int_{\Gamma_{AB}} \frac{\partial}{\partial t}\int_{-\infty}^{\infty} P_S(t + t'\cos\alpha_1, s + t'\sin\alpha_1)\frac{1}{t'}dt'd\theta. \tag{24}$$

For convenience, $\vec{\tau}_1$,t_1,s_1 etc. are shown in Fig. 14(d).

2) Weight function II: $w_S^{II}(\vec{k}) = w_S^{II}(\omega_1\vec{e}_1 + \omega_2\vec{e}_2) = A_S i\mathrm{sgn}(\omega_1)$ with real numbers A_S dependent on the source positions S.

Now, Eq. (17) is simplified as

$$\tilde{P}_S(t,s) = \frac{A_s}{2\pi}\frac{\partial}{\partial t}P_S(t,s). \tag{25}$$

The summed weight function

$$w^{II}(\vec{k}) = \sum_{j=1}^{J(\vec{k})} A_{S^j} i\text{sgn}(\omega_1).$$

Suppose that $w^{II}(\vec{k}) \neq 0$ in the Fourier space. We define

$$W^{II}(\vec{r}) = \int_{R^3} \frac{1}{w^{II}(\vec{k})} \exp(2\pi i\vec{k}\cdot\vec{r})d^3\vec{k}. \tag{26}$$

Eq. (15) becomes

$$\begin{aligned}\Phi^{II}(\vec{r}) &= \frac{1}{2\pi}\int_\Gamma A_s \frac{\partial}{\partial t}P_S(t,s)d\theta \\ \Psi(r) &= \Phi^{II}(\vec{r}) *** W^{II}(\vec{r}).\end{aligned} \tag{27}$$

Since $W^{II}(\vec{r})$ is generally a 3D function, to reconstruct the object $\Psi(\vec{r})$ we must perform a 3D convolution on the intermediate function $\Phi^{II}(\vec{r})$. To obtain a formula which is suitable to reconstruct a part of the object, one needs to adjust the constant A_S so that the summed weight function $w^{II}(\vec{k})$ is reduced to a 1D or 2D function and the 3D convolution is reduced to a 1D or 2D convolution. In a general sense, this remains an open problem.

Fortunately, in the special case of the simple complete curve Γ_{AB} (Fig. 14a), one can take $A_S = 1$. According to Eq. (23) one has

$$\sum_{j=1}^{J_{\vec{k}}} \text{sgn}(\omega_1) = \sum_{j=1}^{J_{\vec{k}}} \text{sgn}(\vec{k}\cdot\vec{e}_1(S^j)) = \text{sgn}(\vec{k}\cdot\vec{e}_\pi).$$

Therefore, we obtain the summed weighted function and the second-step convolution kernel as

$$\begin{aligned}w^{II1}(\vec{k}) &= \sum_{j=1}^{J_{\vec{k}}} w_{S^j}^{II1}(\vec{k}) = \sum_{j=1}^{J_{\vec{k}}} i\text{sgn}(\omega_1) = i\text{sgn}(\vec{k}\cdot\vec{e}_\pi) \\ \frac{1}{w^{II1}(\vec{k})} &= -i\text{sgn}(\vec{k}\cdot\vec{e}_\pi), \\ W^{II1}(\vec{r}) &= \int_{R^3} -i\text{sgn}(\vec{k}\cdot\vec{e}_\pi)\exp(i2\pi\vec{k}\cdot\vec{r})d^3\vec{r} = \tfrac{1}{\pi t'}\delta(t_1')\delta(t_2'),\end{aligned}$$

where $t' = \vec{r}\cdot\vec{e}_\pi, t_1' = \vec{r}\cdot\vec{e}_{\pi 1}, t_2' = \vec{r}\cdot\vec{e}_{\pi 2}$, and $\vec{e}_{\pi 1}, \vec{e}_{\pi 2}, \vec{e}_\pi$ are three orthogonal normal vectors. Therefore, Eq. (27) becomes

$$\Phi^{II1}(\vec{r}) = \frac{1}{2\pi}\int_{\Gamma_{AB}} \frac{\partial}{\partial t}P_S(t,s)d\theta$$

$$\Psi(\vec{r}) = -\int_{-\infty}^{\infty} \Phi^{II1}(\vec{r} + t'\vec{e}_\pi)\frac{1}{\pi t'}dt' \tag{28}$$

where the 1D convolution is performed. This formula is also suitable to reconstruct a part of the object from truncated data, because one just needs to calculate locally the intermediate function $\Phi^{II1}(\vec{r}+t'\vec{e}_\pi)$, on the line through the point $\vec{r}$ and along the direction $\vec{e}_\pi$.

3) Weight function III $w_S^{III}(\vec{k}) = w_S^{III}(\omega_1\vec{e}_1 + \omega_2\vec{e}_2) = \frac{A_S}{|\omega_1|}$.

Equation (17) becomes

$$\tilde{P}_S^{III}(t,s) = A_S \int_{R^2} \exp(2\pi i(\omega_1 t + \omega_2 s))\widehat{P}_S(\omega_1,\omega_2)d\omega_1 d\omega_2 = A_S P_S(t,s). \tag{29}$$

Then, we obtain a backprojection algorithm as

$$\begin{aligned} \Phi^{III}(\vec{r}) &= \int_\Gamma A_S P_S^{III}(t,s)d\theta, \\ \widehat{\Phi}(\vec{k}) &= \widehat{\Psi}(\vec{k})w^{III}(\vec{k}), \end{aligned} \tag{30}$$

where $w^{III}(\vec{k}) = \sum_{j=1}^{J_{\vec{k}}} A_{S^j}|\omega_1|^{-1} = \sum_{j=1}^{J_{\vec{k}}} A_{S^j}|\vec{k}\cdot\vec{e}_1(S^j)|^{-1}$.

The first step $P_S^{III}(t,s) \to \Phi^{III}(\vec{r})$ is localized but the second step $\Phi^{III}(\vec{r}) \to \Psi(\vec{r})$ is not local unless the curve Γ is properly specialized, such as the great circle of the unit sphere. The convenient way is to view $\Phi^{III}(\vec{r})$ as an approximate local reconstruction formula and omit the second step.

4) Weight function IV $w_S^{IV}(\vec{k}) = w_S^{IV}(\omega_1\vec{e}_1 + \omega_2\vec{e}_2) = A_S|\omega_1|$.

Equation (17) becomes

$$\begin{aligned} \tilde{P}_S^{IV}(t,s) &= A_S \int_{R^2} \exp(2\pi i\vec{k}\cdot\vec{r})\widehat{P}_S(\omega_1,\omega_2)\omega_1^2 d\omega_1 d\omega_2 \\ &= -\tfrac{1}{4\pi^2}A_S\tfrac{\partial^2}{\partial t^2}P(t,s). \end{aligned} \tag{31}$$

Then, we obtain the lambda-type local reconstruction formula

$$\begin{aligned} \Phi^{IV}(\vec{r}) &= -\frac{1}{4\pi^2}\int_\Gamma A_S\frac{\partial^2}{\partial t^2}P_S(t,s)d\theta, \\ \widehat{\Phi}^{IV}(\vec{k}) &= \widehat{\Psi}(\vec{k})w^{IV}(\vec{k}), \end{aligned} \tag{32}$$

where $w^{IV}(\vec{k}) = \sum_{j=1}^{J_{\vec{k}}} A_{S^j}|\omega_1| = \sum_{j=1}^{J_{\vec{k}}} A_{S^j}|\vec{k}\cdot\vec{e}_1(\vec{S}^j)|$.

Similarly, the convenient way is to view $\Phi^{IV}(\vec{r})$ as an approximate local reconstruction and omit the second step.

5) Weight function V: $w_S^V(\vec{k}) = w_S^V(\omega_1\vec{e}_1 + \omega_2\vec{e}_2) = 1$.

The weight function is 1 for every point on the frequency plane. The summed weight function is

$$w^V(\vec{k}) = \sum_{j=1}^{J(\vec{k})} w_{S^j}^V(\vec{k}) = J(\vec{k}).$$

Eq. (17) is simplified as

$$\tilde{P}_S^V(t,s) = \frac{1}{2\pi}\frac{\partial}{\partial t}\int_{R^2} \exp(2\pi i(\omega_1 t + \omega_2 s)\widehat{P}_S(\omega_1,\omega_2)(-i)\mathrm{sgn}(\omega_1)d\omega_1 d\omega_2$$
$$= -\frac{1}{2\pi}\frac{\partial}{\partial t}\int_R P_S(t+t',s)\frac{1}{\pi t'}dt'. \tag{33}$$

The reconstruction formula (15) becomes

$$\Phi^V(\vec{r}) = -\frac{1}{2\pi}\int_\Gamma \frac{\partial}{\partial t}\int_R P_S(t+t',s)\frac{1}{\pi t'}dt'd\theta$$
$$\Phi^V(\vec{k}) = \widehat{\Psi}(\vec{k})J(\vec{k}). \tag{34}$$

On the projection plane, the convolution in Eq. (34) is performed along the tangential direction of the curve Γ at S. If Γ is half a great circle on the unit ball, the frequency point is scanned by the frequency plane exactly once, $J(\vec{k}) = 1$, $\Phi^V(\vec{r})$ is an exact reconstruction of the object function, i.e., $\Phi^V(\vec{r}) = \Psi(\vec{r})$. If the curve Γ is close to half a great circle so that $J(\vec{k}) = 1$ in the main part of the Fourier domain and $J(\vec{k})$ equals an integer close to 1 in the rest part, $\Phi^V(\vec{r})$ is a good approximation of the object function, $\Phi^V(\vec{r}) \approx \Psi(\vec{r})$. Otherwise, $\Phi^V(\vec{r})$ is no longer a good approximation of $\Psi(\vec{r})$, and the second step filtration is necessary.

For a simple complete curve Γ_{AB}, Formula (34) can be expressed as

$$\Phi^V(\vec{r}) = -\frac{1}{2\pi}\int_{\Gamma_{AB}} \frac{\partial}{\partial t}\int_R P_S(t+t',s)\frac{1}{\pi t'}dt'd\theta$$
$$\Phi^V(\vec{k}) = \widehat{\Psi}(\vec{k})J(\vec{k}).$$

Therefore, the Palamodov's parallel-beam formula

$$\Psi(\vec{r}) = -\frac{1}{2\pi}\int_{\Gamma_{AB}} \frac{\partial}{\partial t}\int_R P_S(t+t',s)\frac{1}{\pi t'}dt'd\theta, \tag{P1}$$

which is referred to as Theorem 3 in paper [36] and Theorem 4.3 in the monograph [37], is generally approximate. In the proof in [37], the flaw is no compensation for the fact that the frequency plane may scan some regions in the frequency space more than once ($J(\vec{k}) > 1$).

5. Cone-beam reconstruction

Similar to the 2D case, let us translate the reconstruction formulae for 3D parallel-beam case to the cone-beam CT with the well-known relations between the parallel- and divergent-beam projections in Fig. 5.

5.1. A trajectory and its complete region

A trajectory C consists of a finite number of curve segments in the 3D space R^3, along which an x-ray source goes (Fig. 15). The cone-beam projection of the object function $\Psi(\vec{r})$ along a trajectory C is defined by

$$p_{S'}(\vec{n}) = \int_0^\infty \Psi(\overrightarrow{OS'} + \vec{n}l)dl$$

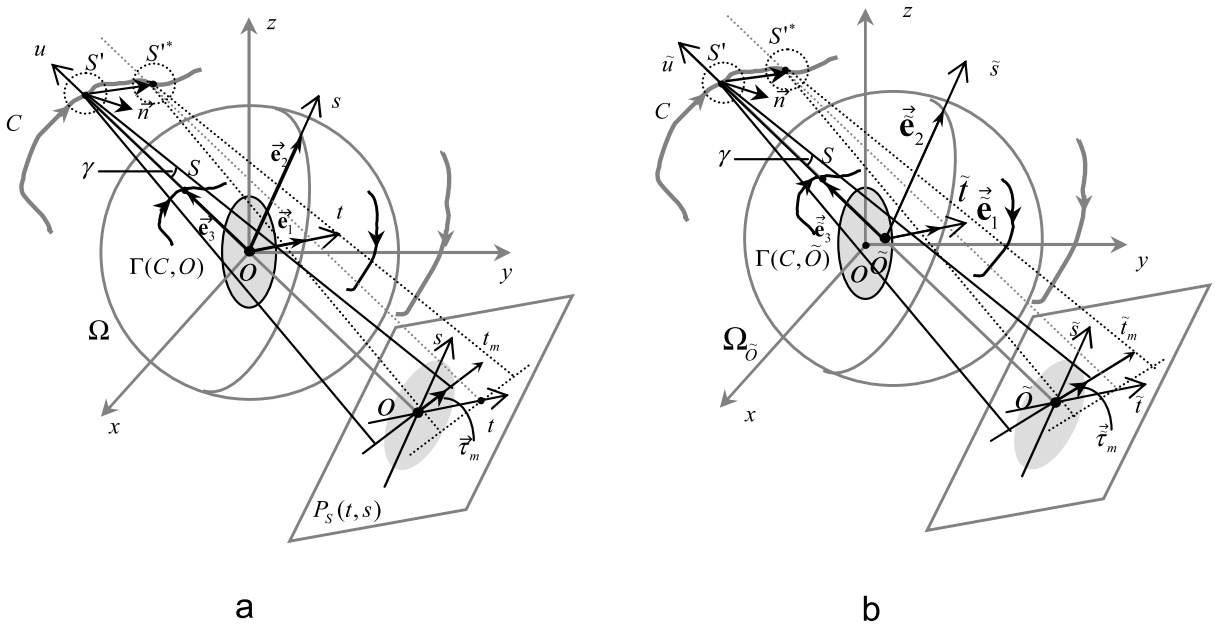

Fig. 15. Imaging geometries for cone-beam reconstruction at points O (a) and $\tilde{O}$ (b) from data collected along a general trajectory C.

for all $S' \in C$, and $\vec{n} \in \Omega$.

In R^3, the unit sphere centered at a point $\tilde{O}$ is defined as

$$\Omega_{\tilde{O}} = \left\{ S \in R^3 : |\overrightarrow{\tilde{O}S}| = |\vec{\tilde{e}}_3| = 1 \right\}.$$

For a point $\tilde{O} \notin C$, the projection of the locus C on the unit sphere $\Omega_{\tilde{O}}$ is defined as

$$\Gamma(C, \tilde{O}) = \left\{ S \in \Omega_{\tilde{O}} : \overrightarrow{\tilde{O}S} = \overrightarrow{\tilde{O}S'}/|\overrightarrow{\tilde{O}S'}|, S' \in C \right\}.$$

If $\Gamma(C, \tilde{O})$ is complete on the unit sphere $\Omega_{\tilde{O}}$, we say that the trajectory C is complete with respect to $\tilde{O}$ or that the point $\tilde{O}$ is a complete point of the trajectory$C$. The set of the complete points is called the complete Region of the locus C, denoted as R(C). In contrast to the 2D case, integrals along some lines through a complete point may be unknown. This fact causes some difference between fan- and cone-beam reconstruction.

A special trajectory is the differentiable curve $C_{A'B'}$, which starts from point A' to B' with the chord $A'B'$ through the origin O, see Fig. 16. Clearly, $C_{A'B'}$ is complete with respect to any point between A' and B', but generally incomplete with respect to points beyond the chord $A'B'$.

5.2. Reconstruction formulae for cone-beam CT

Now, we translate the formulae for the parallel-beam to cone-beam case with the three-step method we employed for 2D CT.

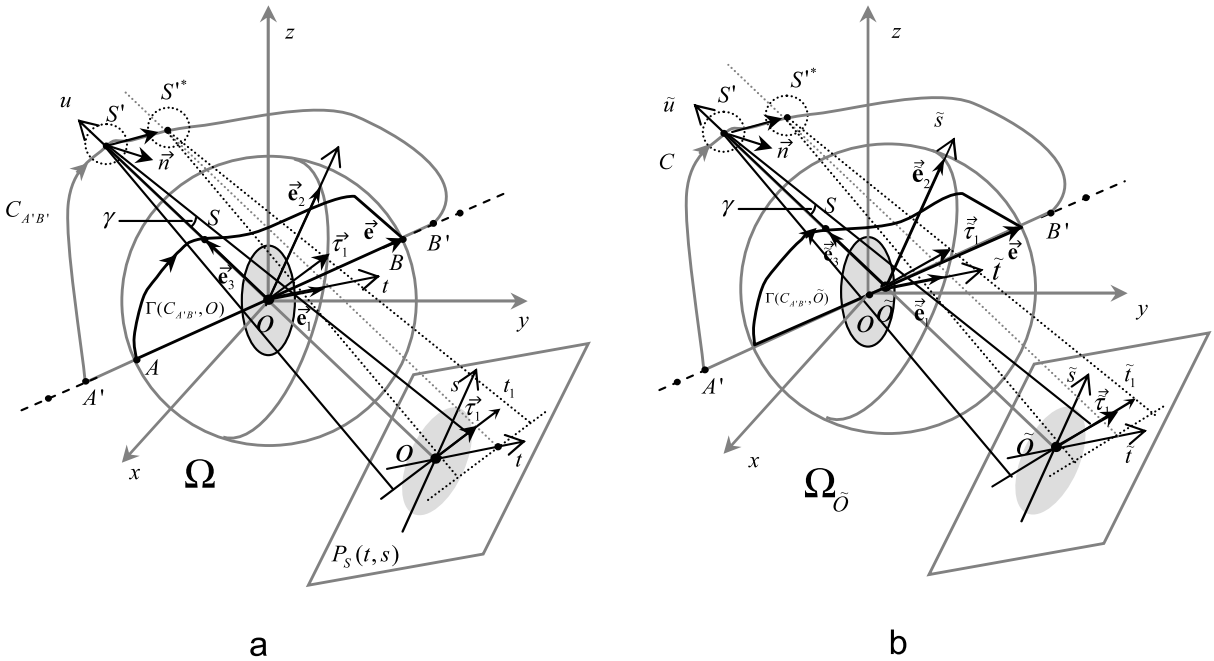

Fig. 16. Imaging geometries for cone-beam reconstruction at points O (a) and $\tilde{O}$ (b) from data collected along the locus $C_{A'B'}$.

5.2.1. The general FBP and its special case

As shown in Fig. 15, for a general trajectory C, without loss of the generality we suppose that O is a complete point, i.e., $O \in R(C)$. In other words, $\Gamma(C, O)$, the projection of C on the unit sphere Ω, is a complete curve. We assume that the parallel-beam projection $P_S(t, s)$ are known for every $S \in \Gamma(C, O)$.

Step 1. For every $S \in \Gamma(C, O)$, the local coordinate system Otsu is defined by the origin O and the three unit vectors, $\vec{e}_3 = \overrightarrow{OS}, \vec{e}_1$ the tangential direction of $\Gamma(C, O)$ at S, and $\vec{e}_2 = \vec{e}_3 \times \vec{e}_1$, as we did in the 3D parallel-beam case.

Equation (22) can be rewritten as

$$\Psi(O) = -\frac{1}{2\pi^2} \int_{\Gamma(C,O)} \frac{\partial}{\partial t}\bigg|_{t=0} \sum_{m=0}^{M-1} c_m \int_{-\infty}^{\infty} P_S(t + t' \cos\alpha_m, t' \sin\alpha_m) \frac{1}{t'} dt' d\theta,$$

where c_m α_m are dependent on $\Gamma(C, O)$.

Step 2. See Fig. 15a. Recall that S' is the intersection point between the half straight line OS and the locus C, i.e., $\overrightarrow{OS'}/|\overrightarrow{OS'}| = \overrightarrow{OS} = \vec{e}_2$. $S'^* \in C$ is another point on the locus near S', whose local coordinates in the system Otsu are

$$t = \overrightarrow{OS'^*} \cdot \vec{e}_1 = \overrightarrow{S'S'^*} \cdot \vec{e}_1, s = \overrightarrow{OS'^*} \cdot \vec{e}_{2,u} = \overrightarrow{OS'^*} \cdot \vec{e}_3.$$

When $t = 0$, the point S'^* coincides with the point S'. When $S'^* \to S', s \to 0$ is faster than $t \to 0$.

In reference to Fig. 5, one has the relation between parallel-beam projection $P_S(t, s)$ and cone-beam projection $p_{S'^*}(\vec{n})$,

$$\int_{-\infty}^{\infty} P_S(t + t' \cos\alpha_m, s + t' \sin\alpha_m) \frac{1}{t'} dt' = \int_{-\infty}^{\infty} p_{S'^*(t,s,u)}(-\vec{e}_3 \cos\gamma + \vec{\tau}_m \sin\gamma) \frac{1}{\sin\gamma} d\gamma,$$

$$P_S(t,s) = p_{S'^*(t,s,u)}(-\vec{e}_3) + p_{S'^*(t,s,u)}(\vec{e}_3),$$

where the unit vector $\vec{\tau}_m = \vec{e}_1 \cos\alpha_m + \vec{e}_2 \sin\alpha_m$.

Then, Eq. (22) becomes

$$\Psi(O) = -\frac{1}{2\pi^2} \int_{\Gamma(C,O)} \frac{d}{dt}\bigg|_{t=0} \int_0^{2\pi} \sum_{m=0}^{M-1} c_m p_{S'^*(t,s,u)}(-\vec{e}_3 \cos\gamma + \vec{\tau}_m \sin\gamma) \frac{d\gamma}{\sin\gamma} d\theta, \tag{35}$$

$c_m, \vec{\tau}_m$ are dependent on $\Gamma(C,O)$. Since the source position $S'^* \in C$ moves along the curve C in R^3, we write the derivation in Eq. (35) as $\frac{d}{dt}\big|_{t=0}$ instead of $\frac{\partial}{\partial t}\big|_{t=0}$.

The derivative operation in Eq. (35) can be explicitly written as

$$\frac{d}{dt}\bigg|_{t=0} \int_0^{2\pi} \sum_{m=0}^{M-1} c_m p_{S'^*(t,s,u)}(-\vec{e}_3 \cos\gamma + \vec{\tau}_m \sin\gamma) \frac{d\gamma}{\sin\gamma}$$

$$= \lim_{S'^* \to S'} \frac{1}{\overrightarrow{S'S'^*} \cdot \vec{e}_1} \int_0^{2\pi} \sum_{m=0}^{M-1} c_m (p_{S'^*}(-\vec{e}_3 \cos\gamma + \vec{\tau}_m \sin\gamma) - p_{S'}(-\vec{e}_3 \cos\gamma + \vec{\tau}_m \sin\gamma)) \frac{d\gamma}{\sin\gamma}.$$

Step 3. For any complete point $\tilde{O} \in R(C)$, the reconstruction formula for cone-beam projection is

$$\Psi(\tilde{O}) = -\frac{1}{2\pi^2} \int_{\Gamma(C,\tilde{O})} \frac{d}{d\tilde{t}}\bigg|_{\tilde{t}=0} \int_0^{2\pi} \sum_{m=0}^{M-1} c_m p_{S'^*(\tilde{t},\tilde{s},\tilde{u})}(-\vec{\tilde{e}}_3 \cos\gamma + \vec{\tilde{\tau}}_m \sin\gamma) \frac{d\gamma}{\sin\gamma} d\theta, \tag{36}$$

where $c_m, \vec{\tilde{\tau}}_m$ are dependent on $\Gamma(C,\tilde{O})$, as shown in Fig. 15(b).

Similarly, the derivative operation in Eq. (36) can be explicitly written as

$$\frac{d}{d\tilde{t}}\bigg|_{t=0} \int_0^{2\pi} \sum_{m=0}^{M-1} c_m p_{S'^*(\tilde{t},\tilde{s},\tilde{u})}(-\vec{\tilde{e}}_3 \cos\gamma + \vec{\tilde{\tau}}_m \sin\gamma) \frac{d\gamma}{\sin\gamma}$$

$$= \lim_{S'^* \to S'} \frac{1}{\overrightarrow{S'S'^*} \cdot \vec{\tilde{e}}_1} \int_0^{2\pi} \sum_{m=0}^{M-1} c_m (p_{S'^*}(-\vec{\tilde{e}}_3 \cos\gamma + \vec{\tilde{\tau}}_m \sin\gamma) - p_{S'}(-\vec{\tilde{e}}_3 \cos\gamma + \vec{\tilde{\tau}}_m \sin\gamma)) \frac{d\gamma}{\sin\gamma}.$$

The local coordinate system $\tilde{O}\tilde{t}\tilde{s}\tilde{u}$ is defined by the origin$\tilde{O}$, and the three orthonormal vectors $\vec{\tilde{e}}_3 = \overrightarrow{\tilde{O}S}$, $\vec{\tilde{e}}_1$ (the tangential direction of $\Gamma(C,\tilde{O})$ at S), and $\vec{\tilde{e}}_2 = \vec{\tilde{e}}_3 \times \vec{\tilde{e}}_1$. For example, the local coordinates of $S'^* \in C$ are

$$\tilde{t} = \overrightarrow{\tilde{O}S'^*} \cdot \vec{\tilde{e}}_1 = \overrightarrow{S'S'^*} \cdot \vec{\tilde{e}}_1, \tilde{s} = \overrightarrow{\tilde{O}S'^*} \cdot \vec{\tilde{e}}_2, \tilde{u} = \overrightarrow{\tilde{O}S'^*} \cdot \vec{\tilde{e}}_3.$$

Formula (36) is a general cone-beam FBP formula, which does not need the assumption that the object must be supported inside the trajectory. When the trajectory is a finite union of C^∞-curve, this formula coincides with the Katsevich's general scheme [21].

In the following, we directly give the associated cone-beam reconstruction formulae without describing the corresponding three steps. For the cone-beam trajectory $C_{A'B'}$ (Fig. 16) and any point on the chord $A'B'$, i.e., $\tilde{O} \in (A', B')$, using the three step-method, the reconstruction formula (24) can be obtained as

$$\Psi(\tilde{O}) = -\frac{1}{2\pi^2} \int_{\Gamma(C_{A'B'},\tilde{O})} \frac{d}{d\tilde{t}}\bigg|_{\tilde{t}=0} \int_0^{2\pi} p_{S'^*(\tilde{t},\tilde{s},\tilde{u})}(-\vec{e}_3 \cos\gamma + \vec{\tilde{\tau}}_1 \sin\gamma) \frac{d\gamma}{\sin\gamma} d\theta,$$

with $\vec{\tilde{\tau}}_1 = \left(\vec{e}_\pi - (\vec{e}_\pi \cdot \vec{\tilde{e}}_3)\vec{e}_\pi\right) \Big/ |\vec{e}_\pi - (\vec{e}_\pi \cdot \vec{\tilde{e}}_3)\vec{e}_\pi|, \;\; \vec{e}_\pi = \overrightarrow{A'B'}/|\overrightarrow{A'B'}|$.

This formula is consistent with the filtered backprojection formulae (FBP) developed by several groups [13–17].

5.2.2. The general BPF and its special case

For any complete point $\tilde{O}$ of a general trajectory C, i.e., $\tilde{O} \in R(C)$, based on Eq. (27), the intermediate function $\Phi^{II}(\tilde{O})$ can be calculated from

$$\Phi^{II}(\tilde{O}) = \frac{1}{2\pi} \int_{\Gamma(C,\tilde{O})} A_S \frac{d}{d\tilde{t}}\bigg|_{\tilde{t}=0} \left(p_{S'^*(\tilde{t},\tilde{s},\tilde{u})}(\vec{\tilde{e}}_3) + p_{S'^*(\tilde{t},\tilde{s},\tilde{u})}(-\vec{\tilde{e}}_3)\right) d\theta.$$

However, generally speaking, it is an open question how to reconstruct the object function $\Psi(\tilde{O})$ from $\Phi^{II}(\tilde{O})$.

Fortunately, for the trajectory $C_{A'B'}$ (Fig. 16) and any point on the chord $A'B'$, i.e., $\tilde{O} \in (A', B')$, by Eq. (28) the intermediate function can be calculated by

$$\Phi^{II1}(\tilde{O}) = \frac{1}{2\pi} \int_{\Gamma(C_{A'B'},\tilde{O})} \frac{d}{d\tilde{t}}\bigg|_{\tilde{t}=0} \left(p_{S'^*(\tilde{t},\tilde{s},\tilde{u}))}(\vec{\tilde{e}}_3) + p_{S'^*(\tilde{t},\tilde{s},\tilde{u})}(-\vec{\tilde{e}}_3)\right) d\theta.$$

Though Eq. (28)

$$\Psi(\vec{r}) = -\int_{-\infty}^{\infty} \Phi^{II1}(\vec{r} + t'\vec{e}_\pi) \frac{1}{\pi t'} dt', \tag{37}$$

with $\vec{e}_\pi = \overrightarrow{A'B'}/|\overrightarrow{A'B'}|$ requires the value of $\Phi^{II1}(\tilde{O})$ for all points $\tilde{O}$ on the line $A'B'$, the object function $\Psi(\vec{r})$ at any point $\vec{r}$ between A' and B' can be reconstructed from $\Phi^{II1}(\tilde{O})$ using the so-called finite inverse Hilbert [24,38] if the object function value $\Psi(\vec{r})$ is zero outside the line segment $A'B'$.

This formula is consistent to the backprojection filtration formulae [13,15,18–20]. In [13,18,20], the BPF is introduced based on the odd extension of the projection data. The even extension was introduced in [15] when the framework based on Tuy's formula was set up. However, according to our current understanding, Theorem 3 in [15] is compromised by a minor conceptual flaw. In the proof of Theorem 3 in [15], Eq. (38) holds for $x \in (a_1, a_2)$ instead of on the whole line because of the condition of Eq. (34). It is not permissible to apply the inverse Hilbert transform $H_{a_2-a_1}$ on Eq. (38) to obtain Theorem 3. In other words, there exists an essential difference between the even and odd extensions of projection. We acknowledgement that the minor change of the phase from "the inverse Hilbert transform" to "the finite inverse Hilbert transform" has no influence on the scheme described in [15].

5.2.3. The approximate reconstruction formulae

For any complete point $\tilde{O}$ of a general trajectory C, i.e., $\tilde{O} \in R(C)$, based on the relation between parallel- and divergent-beam projections, an approximate reconstruction function $\Phi^{III}(\tilde{O})$ in Eq. (30) and $\Phi^{IV}(\tilde{O})$ in Eq. (32) can be calculate from the cone-beam projection as well:

$$\Phi^{III}(\tilde{O}) = \int_{\Gamma(C,\tilde{O})} A_S (p_{S'}(\vec{\tilde{e}}_3) + p_{S'}(-\vec{\tilde{e}}_3)) d\theta$$

$$\Phi^{IV}(\tilde{O}) = \frac{-1}{(2\pi)^2} \int_{\Gamma(C,\tilde{O})} A_S \frac{d^2}{d\tilde{t}^2}\bigg|_{\tilde{t}=0} (p_{S'^*(\tilde{t},\tilde{s},\tilde{u})}(\vec{\tilde{e}}_3) + p_{S'^*(\tilde{t},\tilde{s},\tilde{u})}(-\vec{\tilde{e}}_3)) d\theta.$$

It is consistent with the local cone-beam reconstruction formulae developed by Louis, Maass [39] and Katsevich [40], respectively.

According to Eq. (34), for a complete point $\tilde{O} \in R(C)$, one can approximately reconstruct the object by

$$\Phi^V(\tilde{O}) = -\frac{1}{2\pi^2}\int_{\Gamma(C,\tilde{O})} \frac{d}{d\tilde{t}}\bigg|_{\tilde{t}=0} \int_0^{2\pi} p_{S'^*(\tilde{t},\tilde{s},\tilde{u})}(-\vec{\tilde{e}}_3\cos\gamma + \vec{\tilde{e}}_1\sin\gamma)\frac{d\gamma}{\sin\gamma}d\theta. \tag{38}$$

If $\Gamma(C,\tilde{O})$ is half a great circle on the unit sphere $\Omega_{\tilde{O}}$, $\Phi^V(\tilde{O})$ is an exact reconstruction, i.e., $\Phi^V(\tilde{O}) = \Psi(\tilde{O})$. If it is near half a great circle, $\Phi^V(\tilde{O})$ is an approximation of the object, $\Phi^V(\tilde{O}) \approx \Psi(\tilde{O})$. For the locus $C_{A'B'}$ and a circular locus, Eq. (38), as an approximate reconstruction formula, coincides with the Palamodov cone-beam reconstruction formula [36,37] and Feldkamp formula [41,42], respectively.

Using the three-step method, the Palamodov parallel-beam reconstruction formula (P1) can be translated into the cone-beam case [36,37]:

$$\Psi(\tilde{O}) = -\frac{1}{2\pi^2}\int_{\Gamma(C_{A'B'},\tilde{O})} \frac{d}{d\tilde{t}}\bigg|_{\tilde{t}=0} \int_0^{2\pi} p_{S'^*(\tilde{t},\tilde{s},\tilde{u})}(-\vec{\tilde{e}}_3\cos\gamma + \vec{\tilde{e}}_1\sin\gamma)\frac{d\gamma}{\sin\gamma}d\theta,$$
$$\tilde{O} \in (A', B'). \tag{P2}$$

Evidently, the approximation in the Palamodov cone-beam Formula (P2) comes from the approximation of the associated parallel-beam formula (P1). After we [43] pointed out the approximate nature of the Palamodov cone-beam formula [36], he modified his proof [44,45]. However, based on our new general reconstruction scheme, it is Theorem 3 in his paper [36] that leads to the approximate nature of his cone-beam formula. Also, we recognize that except for the minor flaw related to the multiple scan of the frequency plane, Palamodov's idea to link the parallel-beam problem to the cone-beam problem is very valuable.

6. Discussions and conclusion

Evidently, we can extend the above discussion into the higher dimensional space to form a reconstruction theory based on truncated projections. This is a promising direction of integral geometry [37]. We are working along this line and will report our results later.

It is necessary to underline the differences between our and others' approaches. Since cone-beam CT is practically important, most researchers have paid much more attention on cone-beam CT in hope to solve the cone-beam problems directly. This makes 3D CT problems quite different from and much more difficult than its 2D counterparts. On the other hand, in this paper 3D parallel-beam problems are first carefully studied, and then cone-beam solutions come out in an easy way through the simple relations between parallel- and divergent-beam projection, as illustrated in Fig. 17. This new methodology is a primary part of the originality of this paper.

The three schemes in the CT field have come from the three different fundamental formulae: Radon's, Tuy's and our new formula (14). However, since the three formulae are related to the different forms of the inverse Fourier transform, these three schemes should be essentially equivalent. The reader needs to choose the convenient one for their problems. Meanwhile it is acknowledged that our scheme can generate many formulae in CT, but not all of them. For example, it is difficult to generate the BPF

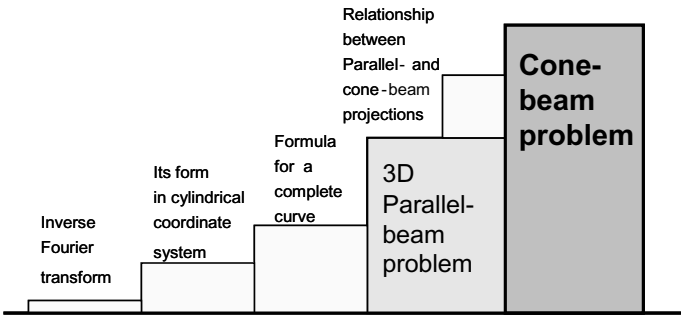

Fig. 17. Steps towards the solution of the cone-beam problem in our scheme.

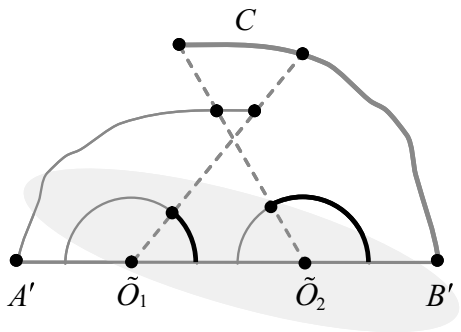

Fig. 18. Applicability of our scheme in the cases of discontinuous trajectories. The traditional assumption that an object be compactly supported inside the locus is no longer necessary.

formula with the odd data extension in [13] and the fan-beam formulae in [46–48]. Hence the reader still needs to pay attention to new methods and results in the CT field.

In conclusion, we have presented an intuitive and complete scheme for CT in different imaging geometries including 2D and 3D parallel- and divergent-beams. A key step is the development of a new fundamental formula starting from the inverse Fourier transform in **cylindrical** coordinate system. Our results have been demonstrated to be not only consistent with the most latest main formulae but also valid under more general conditions including a non-continuous scanning trajectory and an extended object support (Fig. 18). Meanwhile, some minor conceptual flaws in the CT literature have been identified and fixed. Finally, some open questions have been suggested. Our understanding is that Fourier analysis should be viewed as the theoretical foundation of CT and that this complete scheme of CT is just another example among many applications of Fourier analysis in modern sciences and technologies [49].

The authors thank Prof. Y. Ye with University of Iowa for insightful discussions. This work is partially supported by NIH/NIBIB (Grants EB002667, EB004287, EB007288, EB001685 and EB006036) and Ge Healthcare.

Appendix A: An intuitive analogy of the weight function $w_S^{I1}(\omega_1, \omega_2)$

Here we explain how we define this weight function and why it is normal.

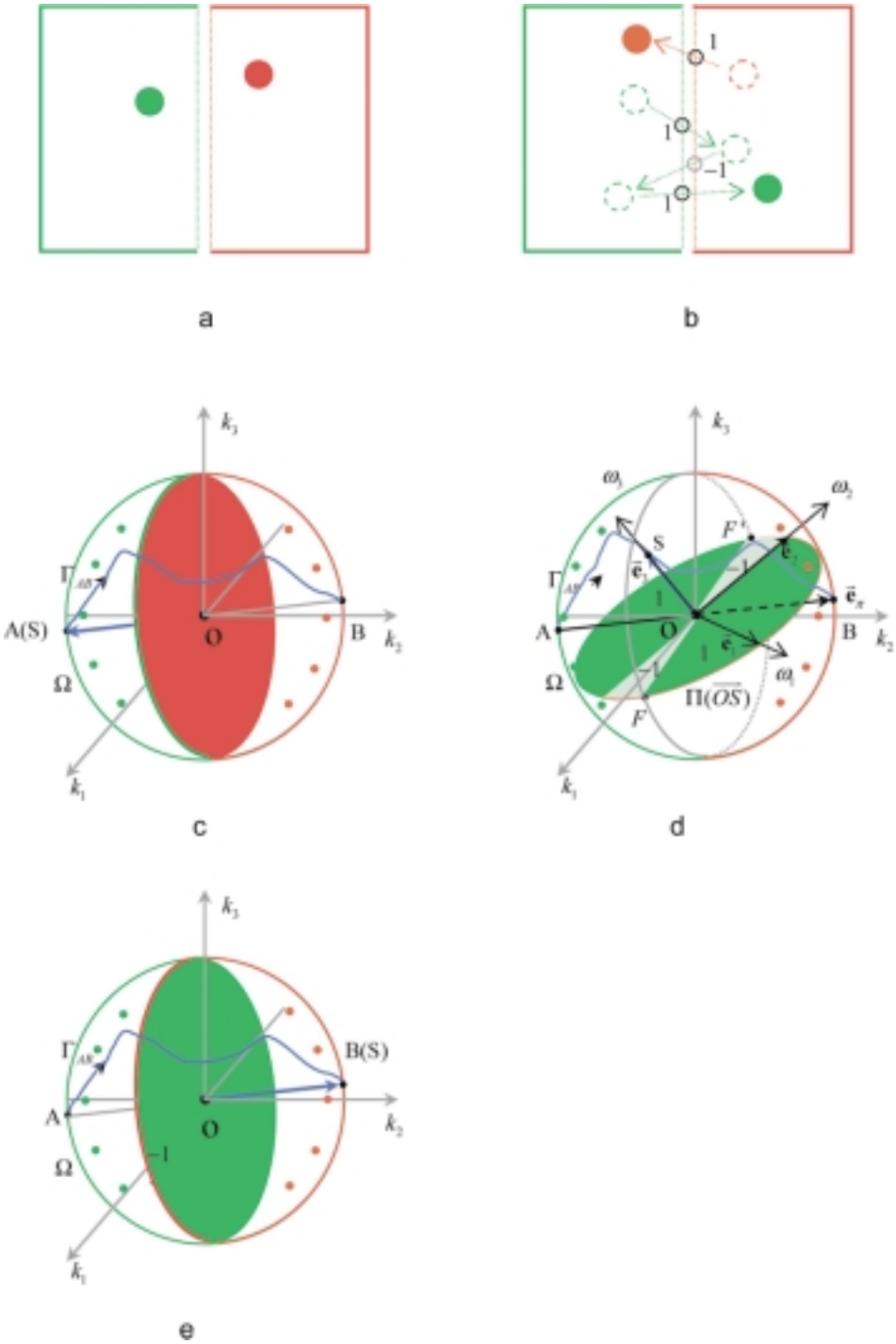

Fig. 19. Analogy of the weight function .Two colored balloon (red and green) have respectively moved from their original (a) to opposite sides (b). A disk inside a sphere turned over from its original position (c) via an intermediate position (d) to the opposite position (e).

1. Outward-homeward function for colored balloons in a room

A red balloon and a green balloon were respectively placed on the red and green sides of a room (Fig. 19a). The two balloons can move inside the room and pass the two middle border lines freely. After some time, the two balloons is found to be on the opposite sides (Fig. 19b). A conclusion can be made that each balloon has effectively passed the border lines only once, no matter how many times the balloon really went over the border lines.

Mathematically, one can define an outward-homeward function to indicate the motion direction of a balloon across the border lines, which takes 1 (outward) when the balloon is going to the other side, and takes -1 (homeward) when it is returning its original side. Note that when a balloon is going to the other side, its color is the same as the color of the first border line it comes across; when it is returning, its color is different from the color of the first border line it sees. If we call the red and green color positive and negative respectively, i.e., sgn(red) $= 1$ and sgn(green) $= -1$, the outward-homeward function can be expressed as

$$\text{sgn(the color of a balloon)} \cdot \text{sgn(the color of the first border line the balloon comes across)}.$$

If a balloon is observed on the opposite side, the sum of the outward-homeward function must be 1, such as $1 - 1 + 1 = 1$ for the green balloon in Fig. 19b.

2. Outward-homeward function for color beads inside a ball

Now, let us imagine that a ball which is divided into two halves by a virtual disk, one half being full of tiny red beads the other full of tiny green beads. The two sides of the disk are red and green accordingly. At the beginning (Fig. 19c), the normal direction of the disk $\overrightarrow{OS}$ was towards to the point A. Then, one moved S along a curve Γ_{AB} on the sphere to point B (Fig. 19d), which is opposite to the point A. During the movement, the ball along with its beads has been kept still and the virtual disk can sweep the beads freely (without any interaction). One can conclude that the disk has passed every bead (either red or green) **effectively only once**. Figure 19e shows an intermediate instant during the disk rotation. The outward-homeward function for the bead being scanned by the disk is identical to the weight function $w_S^{I1}(\omega_1, \omega_2)$:

$$\begin{aligned}&\text{sgn(the color of a bead)sgn(the color the bead see when the disk comes over)}\\&= \text{sgn}(\vec{k} \cdot \vec{e}_\pi)\text{sgn}(\vec{k} \cdot \vec{e}_1) = w_S^{I1}(\omega_1, \omega_2).\end{aligned}$$

In fact, Fig. 19e is a color version of Fig. 14a.

References

[1] G. Hounsfield, Computerized transverse axial scanning (tomography): Part I. Description of system, *British Journal of Radiology* **46** (1973), 1016–1022.

[2] A.C. Kak et al., *Principles of Computerized Tomography Imaging*, SIAM, Philadelphia, 2001.

[3] H. Barrett and W. Swindell, *Radiological Imaging*, Academic, New York, 1981.

[4] A.G. Ramm and A.I. Katsevich, *The Radon Transform and Local Tomography*, CRC, New York, 1996.

[5] J. Radon, Uber die Bestimmung von Funktionnen durch ihre Integralwerte l¨angs gewisser Mannigfaltigkeiten, *Ber Verh Sachs Akad Wiss Leipzig- Math -Natur* **69** (1917), 262–277.

[6] R.N. Bracewell and A.C. Riddle, Inversion of Fan-Beam Scans in Radio Astronomy, *Astrophys J* **150** (1967), 427–434.

[7] G. Herman and A. Naparstek, Fast Image Reconstruction Based on a Radon Inversion Formula Appropriate for Rapidly Collected Dat, *SIAM J Applied Mathematics* **33** (1977), 511–533.

[8] B. Smith, Image reconstruction from cone-beam projections, *IEEE Trans Med Imaging* **4** (1985), 14–25.
[9] P. Grangeat, Mathematical framework of cone beam 3d reconstruction via the 1st derivative of the Radon-transform, *Lecture Notes in Mathematics* **1497** (1991), 66–97.
[10] A. Katsevich, Theoretically exact filtered backprojection-type inversion algorithm for spiral CT, *SIAM J Appl Math* **62** (2002), 2012–2026.
[11] A. Katsevich, Improved exact FBP algorithm for spiral CT, *Adv Appl Math* **32** (2004), 681–697.
[12] G. Wang et al., Approximate and exact cone-beam reconstruction with standard and non-standard spiral scanning, *Phys Med Biol* **52** (2007), R1–R13.
[13] Y. Zou and X. Pan, An extended data function and its generalized backprojection for image reconstruction in helical cone-beam CT, *Phys Med Biol* **49** (2004), N383–N387.
[14] Y. Zou and X. Pan, Image reconstruction on PI-lines by use of filtered backprojection in helical cone-beam CT, *Phys Med Biol* **49** (2004), 2717–2731.
[15] S. Zhao, H. Yu and G. Wang, A unified framework for exact cone-beam reconstruction formulas, *Med Phys* **32**(6) (2005), 1712–1721.
[16] Y. Ye and G. Wang, Filtered backprojection formula for exact image reconstruction from cone-beam data along a general scanning curve, *Med Phys* **32** (2005), 42–48.
[17] J. Pack and F. Noo, Cone-beam reconstruction using 1D filtering along the projection of M-lines, *Inverse Problems* **21** (2005), 1105–1120.
[18] Y. Zou and X. Pan, Exact image reconstruction on PI-lines from minimum data in helical cone-beam CT, *Phys Med Biol* **49** (2004), 941–959.
[19] J.D. Pack, F. Noo and R. Clackdoyle, Cone-beam reconstruction using the backprojection of locally filtered projections, *IEEE Trans Med Imag* **24** (2005), 70–85.
[20] Y. Ye et al., A General Exact Reconstruction for Cone-Beam CT via Backprojection-Filtration, *IEEE Trans Med Imag* **24** (2005), 1190–1198.
[21] A. Katsevich, A general scheme for constructing inversion algorithms for cone-beam CT, *Int J Math Math Sci* **21** (2003), 1305–1321.
[22] F. Noo et al., Image reconstruction from fan-beam projections on less than a short scan, *Phys Med Biol* **47** (2002), 2525–2546.
[23] G. Chen, A new framework of image reconstruction from fan beam projections, *Med Phys* **30** (2003), 1151–1161.
[24] F. Noo et al., A two-step Hilbert transform method for 2D image reconstruction, *Physics In Medicine And Biology* **49**(17) (2004), 3903–3923.
[25] R. Clackdoyle and F. Noo, A large class of inversion formulae for 2D Radon transform of functions of compact support, *Inverse Problems* **20** (2004), 1281–1291.
[26] G. Chen, An alternative derivation of Katsevich's cone-beam reconstruction formula, *Med Phys* **30** (2003), 3217–3226.
[27] H.K. Tuy, An inversion formula for cone-beam reconstruction, *SIAM J Appl Math* **43** (1983), 546–552.
[28] M. Defrise et al., Image reconstruction from truncated, two dimensional, parallel projections, *Inverse Problems* **11** (1995), 287–313.
[29] G. Chen, A new data consistency condition for fan beam projection, *Med Phys* **32** (2005), 961–967.
[30] Y. Wei et al., Integral invariants for Computed tomography, *IEEE Signal Processing Letters* **13** (2006), 549–553.
[31] H. Yu and G. Wang, A general formula for fan-beam lambda tomography, *Int J Biomed Imaging* **2006** (2006), 10427.
[32] H. Yu, Y. Wei, Y. Ye and G. Wang, Lambda tomography with discontinuous scanning trajectories, *Phys Med Biol* **52** (2007), 4331–4344.
[33] S. Orlov, Theory of three dimensional reconstruction I: Conditions for a complete set of projections, *Sov Phys Crystallogr* **20** (1975), 312–314.
[34] S. Orlov, Theory of three dimensional reconstruction: II. The recovery operator, *Sov Phys Crystallogr* **20** (1975), 429–433.
[35] I. Richards et al., *Theory of Distributions*, Cambridge University, Cambridge, England, 1990.
[36] V.P. Palamodov, Reconstruction from ray integrals with sources on a curve, *Inverse Problems* **20** (2004), 239–242.
[37] V.P. Palamodov, *Reconstructive Integral Geometry*, Birhauser Verlag, Boston, 2004.
[38] Y. Ye, H. Yu, Y. Wei and G. Wang, *A General Local Reconstruction Approach Based on a Truncated Hilbert Transform*, 2007, 63634.
[39] A.K. Louis and P. Maass, Contour reconstruction in 3D X ray CT, *IEEE Trans Med Imaging* **12** (1993), 764–769.
[40] A. Katsevich, Improved cone beam local tomography, *Inverse Problems* **22** (2006), 627–643.
[41] L.A. Feldkamp et al., Practical cone-beam algorithm, *J Opt Soc Am* **A1** (1984), 612–619.
[42] H. Yu and G. Wang, Feldkamp-type ROI reconstruction from super-short-scan cone-beam data, *Med Phys* **31** (2004), 1357–1362.
[43] H. Yu et al., Studies on Palamodov's algorithm for cone-beam CT along general curves, *Inverse Problems* **22** (2006), 447–460.

[44] V.P. Palamodov, Comment on 'studies on Palamodov's algorithm for cone-beam CT along a general curve', *Inverse Problems* **22** (2006), 1503–1504.
[45] H. Yu et al., Reply to the comment on 'studies on Palamodov's algorithm for cone-beam CT along a general curve', *Inverse Problems* **22** (2006), 1505–1506.
[46] Y. Wei, G. Wang and J. Hsieh, Relation between filtered backprojection algorithm and backprojection algorithm, *IEEE Signal Process Lett* **9** (2005), 633–636.
[47] Y. Wei and G. Wang, New relations between the divergent beam projection and radon transform with applications, *Inverse Problems* (2007), under review.
[48] Y. Wei, J. Hsieh and G. Wang, General formula for fan-beam computed tomography, *Phys Rev Lett* **95** (2005), 258102.
[49] Y. Wei and Q. Zhang, *Common Waveform Analysis: a new and practical generalization of Fourier analysis*, Kluwer, New York, 2000.